

GeoHealth

RESEARCH ARTICLE

10.1029/2022GH000592

Key Points:

- Overexploiting aquifers increases energy costs and lowers economic productivity by increasing human exposure to geogenic neurotoxins
- Over a 100 year future time-frame estimated revenue from agro-export will be less than the costs this activity imposes on the population
- Investing in water treatment substantially lowers costs of deteriorating water quality

Supporting Information:

Supporting Information may be found in the online version of this article.

Correspondence to:

P. S. K. Knappett,
knappett@tamu.edu

Citation: Knappett, P. S. K., Farias, P., Miller, G.

R., Hoogesteger, J., Li, Y.,
MendozaSanchez, I., et al. (2022). A

to arsenic and fluoride from overexploited aquifers. *GeoHealth*, 6, e2022GH000592.

respectively, compared to the base case (S2). The relative NPV of providing . Without drinking water mitigation, S1 and S3 yielded relative NPVs of

<https://doi.org/10.1029/2022GH000592>
systems approach to remediating human exposure

Received 1 FEB 2022
Accepted 31 MAY 2022

Author Contributions:

Conceptualization: P. S. K. Knappett, P. Farias, G. R. Miller, I. Mendoza-Sanchez, R. T. Woodward, H. Hernandez, I. Loza-Aguirre, G. Carrillo, D. Terrell

Data curation: P. S. K. Knappett, H. Hernandez






Formal analysis: P. S. K. Knappett, P. Farias, G. R. Miller, J. Hoogesteger, R. T. Woodward, H. Hernandez

Funding acquisition: P. S. K. Knappett, Y. Li, H. Hernandez, I. Loza-Aguirre

This is an open access article under the terms of the [Creative Commons Attribution-NonCommercial-NoDerivs License](https://creativecommons.org/licenses/by-nc-nd/4.0/), which permits use and distribution in any medium, provided the original work is properly cited, the use is non-commercial and no modifications or adaptations are made.

KNAPPETT ET AL.

A Systems Approach to Remediating Human Exposure to Arsenic and Fluoride From Overexploited Aquifers

P. S. K. Knappett¹ , P. Farias² , G. R. Miller³ , J. Hoogesteger⁴, Y. Li⁵, I. Mendoza-Sanchez⁶, R. T. Woodward⁷, H. Hernandez⁸, I. Loza-Aguirre⁵ , S. Datta⁹, Y. Huang¹, G. Carrillo⁶, T. Roh⁶ , and D. Terrell¹⁰

¹Geology & Geophysics, Texas A&M University, College Station, TX, USA, ²Environmental Health, Instituto Nacional de Salud Pública, Cuernavaca, México, ³Civil & Environmental Engineering, Texas A&M University, College Station, TX, USA, ⁴Water Resources Management, Wageningen University, Wageningen, The Netherlands, ⁵Mines, Metallurgy and Geology Engineering, University of Guanajuato, Guanajuato, México, ⁶Public Health, Texas A&M University, College Station, TX, USA, ⁷Agricultural Economics, Texas A&M University, College Station, TX, USA, ⁸Geomatic and Hydraulic Engineering, University of Guanajuato, Guanajuato, México, ⁹Geological Sciences, University of Texas at San Antonio, San Antonio, TX, USA, ¹⁰Camino de Agua, San Miguel de Allende, México

Abstract In semiarid agricultural regions, aquifers have watered widespread economic development. Falling water tables, however, drive up energy costs and can make the water toxic for human consumption. The study area is located in central Mexico, where arsenic and fluoride are widely present at toxic concentrations in well water. We simulated the holistic outcomes from three pumping scenarios over 100 years (2020–2120); (S1) pumping rates increase at a similar rate to the past 40 years, (S2) remain constant, or (S3) decrease. Under scenario S1, by 2120, the depth to water table increased to 426 m and energy consumption for irrigation increased to 4×10^9 kWh/yr. Arsenic and fluoride concentrations increased from 14 to 46 $\mu\text{g/L}$ and 1.0 to 3.6 mg/L , respectively. The combined estimated IQ point decrements from drinking untreated well water lowered expected incomes in 2120 by 27% compared to what they would be with negligible exposure levels. We calculated the 100-year Net Present Value (NPV) of each scenario assuming the 2020 average crop value to

to arsenic and fluoride from overexploited aquifers. *GeoHealth*, 6, e2022GH000592. -5.96 water footprint ratio of $0.12 \text{ USD/m} \times 10^9$ and $1.51 \times 10^9 \text{ USD}$, respectively, compared to the base case (S2). The relative NPV of providing . Without drinking water mitigation, S1 and S3 yielded relative NPVs of

blanket reverse osmosis treatment, while keeping pumping constant (S2), was $11.55 \times 10^9 \text{ USD}$ and this

© 2022 The Authors. *GeoHealth* published by Wiley Periodicals LLC on

gain increased when combined with decreased pumping (S3). If a high value, low water footprint crop was substituted (broccoli, 1.51 USD/m^3), the net gains from increasing pumping were similar in size to those of implementing blanket drinking water treatment.

Plain Language Summary Groundwater is jointly used by for-profit agriculture and domestic households for drinking water. Although agriculture creates jobs and stimulates investment, preventing the exposure of children to neurotoxins in drinking water generally means a more prosperous future. We calculate falling water tables, rising energy costs, increasing concentrations of naturally occurring neurotoxins, decreasing IQ and earnings for people living in the basin owing to different rates of pumping by agriculture. For the different pumping scenarios, we calculate the increase or decrease in revenue for the agriculture sector. We then calculate the net economic gain from increasing or decreasing pumping rates, growing alternative crops, and treating drinking water to remove the neurotoxins. We found that people's personal incomes will be ever-more reduced by their exposure to higher concentrations of neurotoxins. The benefits of treating water to remove the neurotoxins are much greater than the costs. Furthermore, increasing pumping rates is only profitable over the long term if it is accompanied by growing much higher value and lower water demand crops

1. Introduction

In semiarid regions, aquifers are commonly the most important water source for irrigation and domestic water use. In the global south, there is little public information to inform individual households about the quality of the groundwater they are drinking and the possible related health risks (Nowicki et al., 2020). This is alarming as we know that many aquifers around the world contain toxic concentrations of dissolved geogenic elements such

than are currently being irrigated in the study area. The most urgent issue, at least from an economic growth perspective, is not limiting pumping but rather treating the drinking water.

Investigation: P. S. K. Knappett, P. Farias, J. Hoogesteger, I. MendozaSanchez, R. T. Woodward, H. Hernandez

Methodology: P. S. K. Knappett, P. Farias, G. R. Miller, Y. Li, R. T. Woodward, H. Hernandez, Y. Huang, T. Roh, D. Terrell

Project Administration: P. S. K. Knappett

Resources: P. S. K. Knappett, R. T. Woodward, H. Hernandez, D. Terrell

Software: P. S. K. Knappett

Supervision: P. S. K. Knappett, R. T. Woodward

Visualization: P. S. K. Knappett, R. T. Woodward, H. Hernandez

Writing – original draft: P. S. K. Knappett

Writing – review & editing: P. S. K. Knappett, P. Farias, G. R. Miller, J. Hoogesteger, Y. Li, I. Mendoza-Sanchez, R. T. Woodward, H. Hernandez, I. LozaAguirre, S. Datta, G. Carrillo, T. Roh, D. Terrell

as arsenic (As) and fluoride (F) (Amini et al., 2008a, 2008b; Nordstrom, 2002; Smedley & Kinniburgh, 2002). Specifically, areas that overlie subduction or rift zones with shallow geothermal heat and little rain commonly have toxic levels of both As and F. Examples are found within Central and South America, the Main Ethiopian Rift Valley, and Central China (Alarcon-Herrera et al., 2013, 2019; Bundschuh et al., 2010; Rango et al., 2013; Xing et al., 2022).

Not only is water quality information rarely provided to the consumers of groundwater, regular monitoring programs that publicly report their findings are generally absent. The lack of maps that detail physical

hydraulic properties of the aquifers and their water chemistry makes it difficult for water managers to anticipate changes to water quality within the world's overexploited aquifers. Ignoring these costs may lead to miscalculating the overall benefit to semiarid and arid regions by engaging in agro-export. Measuring long-term well water chemistry trends is costly and requires sustained funding that typically only well-funded government agencies in rich countries possess. Decades of monitoring by the United States Geological Survey's National Water-Quality Assessment Program revealed the tendency for As concentrations to rise in production wells with high pumping rates (Ayotte et al., 2011). To the authors' knowledge, nothing at this scale has been executed in the developing world.

When an aquifer is overexploited, the economic costs noticed by stakeholders are increasing drilling and pumping costs to access the falling water table. The rate at which these costs increase over time tends to be linear and therefore predictable. A second economic impact, however, is rarely accounted for in decision-making: water quality deterioration as a function of overexploitation. This process directly relates to socio-economic costs of public health and productivity of the regional labor force. We hypothesize that a more complete accounting of how each sector impacts and is impacted by the common pool resource of potable groundwater will permit the optimization of these resources for all stakeholders (Harou & Lund, 2008; Ostrom, 1990).

Therefore, the goal of this study is to simulate the costs, benefits, and Net Present Values (NPVs) of different pathways forward for populations depending on heavily exploited aquifer systems with geogenic contaminants. NPVs are used to economically compare the various scenarios over a 100-year time period. Future costs and benefits are expressed in dollars and discounted to give more weight to near-term consequences than those occurring far in the future. This reflects human preferences and the opportunity costs of money. Commonly used discount rates range from 3% to 5% per year (Carter & Nesbitt, 2016), though rates as low as 1% have been used for very long-term analyses (Stern, 2007).

To account for economic and noneconomic tradeoffs, we developed an innovative hydrologic-public health-economic system dynamics model that builds on concepts introduced in previously published socio-economic-hydrologic models (Elshafei et al., 2015; Harou et al., 2009; Srinivasan et al., 2010). The goals for building these past models include simulating tradeoffs between risks of crop failure versus short-term profit in the context of a shallow salinizing aquifer-river system to help inform the farmer's crop choice (Lefkoff & Gorelick, 1990); estimating the relative dominance of opposing feedbacks between economic growth and environmental degradation on the one hand (positive feedback loop) and human community sensitivity to their environment and ecosystem health on the other (negative feedback loop) (Elshafei et al., 2015); and modeling household water sourcing behavior and their impacts on the water table during a drought underlying a megacity (Srinivasan et al., 2010).

Whereas the link between groundwater scarcity and quality has been explicitly studied in several of these models, the economic impacts of the water quality deterioration has mainly focused on the reduction in crop yield (Lefkoff & Gorelick, 1990) or increased costs for desalinization of irrigation water (Cai, 2008). To the authors' knowledge, no hydrologic-economic study has explicitly modeled the impacts of deteriorating water quality on human health. In this simulation study, we explore the tradeoffs between revenue generated through groundwater pumping for agro-export crops and the water supply and quality, energy demands for pumping, human health, and the economic costs that this activity imposes on the local population who consumes the water. These impacts are presented in their native units (e.g., meters, mg/L, kWh, IQ point decrements, and USD) as well as in discounted economic terms (USD) over the 2020–2120 planning horizon for comparison.

The two principal contaminants of concern considered from a human health perspective are geogenically and geothermally sourced dissolved As and F (Knappett et al., 2020; LaFayette et al., 2020). Both of these contaminants cause a wide range of serious and deadly diseases (Argos et al., 2010; Ayooob & Gupta, 2006; Sage et al., 2017). Arsenic is a carcinogen and also causes vascular diseases. Low levels of F in water are beneficial for

reducing cavities (Rosin-Grget et al., 2013; WHO, 2019), but higher levels of exposure drives tooth and skeletal fluorosis especially in children with developing bones (Ayooob & Gupta, 2006) and may contribute to negative health outcomes in vulnerable adult populations with diabetes and chronic kidney disease (Pratap & Singh, 2013).

Although these health impacts are serious, at the low to medium levels of exposure that are common throughout the study region (10–100 $\mu\text{g/L}$ As, 1–4 mg/L F) (Alarcon-Herrera et al., 2019), the best quantified impacts of these toxins, at present, are the neurotoxic effects on childhood cognitive development (Rocha-Amador et al., 2007; Wasserman et al., 2004, 2014). Exploring the costs of this exposure is relevant since toxic concentrations of As and F commonly co-occur in semiarid and arid regions with shallow geothermal heat (Alarcon-Herrera et al., 2013, 2019; Amini et al., 2008a, 2008b; Ayoob & Gupta, 2006; Bustingorri & Lavado, 2014; Guo et al., 2008; Podgorski et al., 2017, 2018; Rango et al., 2010, 2013; Reyes-Gomez et al., 2013; Saeed et al., 2021; Xing et al., 2022). The concentrations of these toxins in well water may rise over time owing to overexploitation of the aquifers in semiarid and arid regions by pumping for irrigation (Ayotte et al., 2011, 2015; Knappett et al., 2020; Smith et al., 2018). The model presented in this study explicitly calculates IQ point decrements owing to different exposure levels to each toxin and ignores the many serious illnesses caused by these. The model calculates the impacts of exposure to As and F in drinking water on childhood IQ loss and therefore lost income. Published dose-response curves from empirical epidemiology studies are applied to calculate IQ point decrements in the population owing to present-day and predicted As and F concentrations. This approach follows that used to justify the costly phasing out of lead in gasoline by the US EPA (Grosse et al., 2002; Schwartz et al., 1985). This approach was later utilized to calculate lost incomes throughout Low and Middle Income Countries owing to the prolonged period of phasing out lead from gasoline and other products (Attina & Trasande, 2013).

We developed a system dynamics model based on the overexploited Upper Rio Laja Watershed in the state of Guanajuato, central Mexico. Toxic levels of As and F have been present near the water table in this basin at least as far back as the 1990s (Ortega-Guerrero, 2009), but their concentrations appear to be increasing owing to the falling water table and mixing of geothermally influenced waters with shallow meteoric water via long-screened wells (Knappett et al., 2020). We leverage data we have assembled through our diverse teams working in this basin for 10 years. These data include basin-wide demographic data, electricity subsidies, and water governance structures (Hoogesteger & Wester, 2017); irrigation needs for commonly grown crops (Torres Padilla, 2021); historical pumping rates and water table declines (Li et al., 2020); the distribution of As and F concentrations across time and space (Knappett et al., 2020); empirically measured dose-response curves of IQ reduction associated with childhood exposure to varying As and F concentrations in drinking water (Rocha-Amador et al., 2007); and the costs of the two most widely used drinking water mitigation options in Mexico (Del Razo et al., 2018).

In this basin, over 80% of pumped groundwater is used to irrigate mostly agro-export crops. Therefore, outside investors and international market prices drive the majority of the pumping. The objective of this study is to generate new insights into the tradeoffs of different policy interventions in the areas of safe domestic water supply, health, and economic development. Based on past pumping rates of the agriculture sector and to stimulate debate over the benefits of changing the status quo, we developed and ran the model as a simulation with three future pumping scenarios: (S1) pumping continues to increase at a rate consistent with past decades; (S2) pumping rates are unchanged from 2020; and (S3) pumping rates decrease steadily. We then calculate the lift height, water quality, IQ point decrements, energy demand, and economic costs and benefits for the rural households and farms in the basin over a 100-year timeframe with and without mitigation of drinking water. We then varied crop type to reveal the impact of crop value and crop water footprint on the outcome. We summarize the results by comparing the NPV of each pumping and treatment scenario over the next 100 years relative to the baseline S2 pumping scenario with no treatment.

2. Methods and Data

2.1. Description of System Dynamics Model

The model takes into account the impacts of irrigation pumping on lift height, well water As and F concentrations, drinking water quality, child IQ, and household wealth of the residents in an agricultural basin where there is a link between falling water tables and rising concentrations of geogenic contaminants (Figure 1). Lift height, As and F concentrations, population IQ, and household income are all stocks or proxies for stocks in the model (Figure 1). The upstream side of the model (left side) quantifies how irrigation pumping benefits the farms and

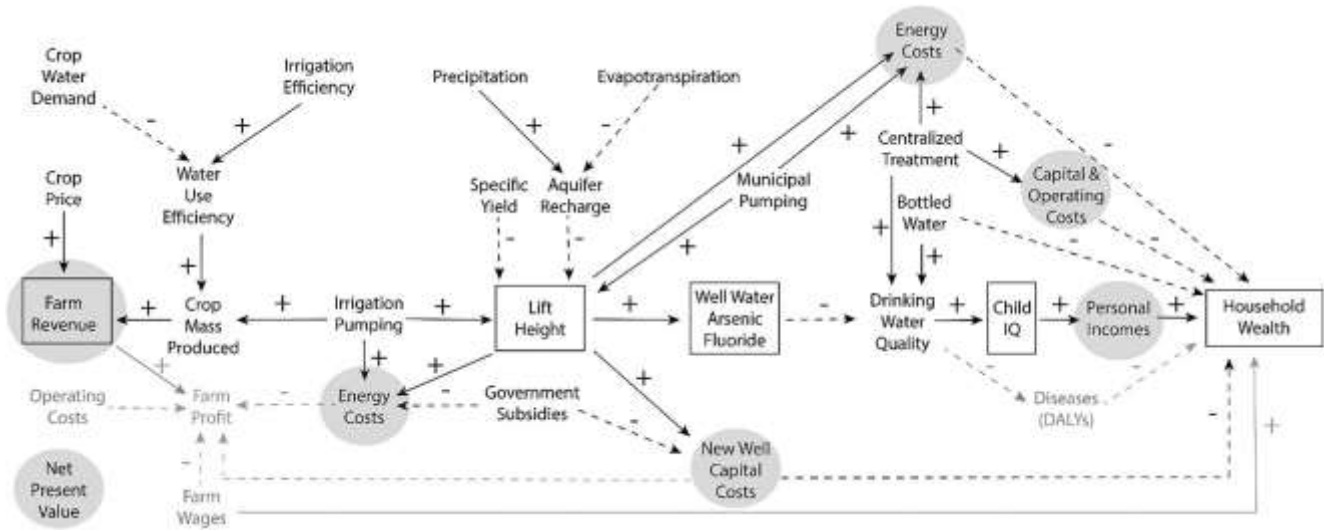


Figure 1. System dynamics model describing the impacts of irrigation pumping on the stocks (black boxes) lift height, well water As and F concentrations, child IQ and household wealth of the residents in an agricultural basin in a semi-arid region. The polarity of the causal relationship is indicated with a + or – sign. Gray flows represent processes and outcomes that are not included in the present study. Gray shaded circles represent economic stocks and flows that were used to calculate the Net Present Value of each simulation scenario.

businesses that pump while simultaneously imposing a cost on themselves in the form of energy costs due to greater lift heights, which cuts into farm profit (Li et al., 2020).

Irrigation pumping imposes two types of costs on all aquifer stakeholders (right side of Figure 1): costs to access the water and costs from consuming the water with deteriorating quality. Costs associated with accessing deep and falling water tables include well modifications (new well drilling, well deepening, and pump replacement or lowering) and energy costs from lifting water to the surface. The second cost is the impaired cognitive development from drinking well water directly or, alternatively, the costs of mitigating exposure to the well water through purchasing bottled water privately or investing in centralized water treatment. This adds to the overall energy costs the community must pay for access to safe water. The increased costs of accessing, consuming, replacing, or treating the water depresses the household wealth.

The pumping scenarios and mitigation options that are considered in the model are described in Table 1. In pumping scenario S1, water tables will continue to fall, electricity costs will rise for farmers, geogenic As and F concentrations will rise, childhood IQ of the population drinking from the aquifer will be reduced, and lifetime earnings in the region will decrease. Thus, pumping for profit will depress the long-term rate of growth of incomes for the general population compared to what that growth could have been if another economic activity with a smaller water demand had generated the same amount of wealth for the local population as the agriculture industry does today. Investments in new irrigation efficiency technologies may enable this region to stabilize the pumping rates (S2) or even reduce them if more efficient irrigation is combined with growth in lower water demand sectors of the economy (S3). The three mitigation approaches considered are (a) bottled water paid for by individual households, (b) centralized water treatment paid for by a community (0% subsidy), and (c) centralized water treatment paid for by state and federal government (100% subsidy).

Table 1
Pumping Scenarios and Mitigation Options Considered in the System Dynamics Model

Pumping scenario ID	Description	Mitigation ID	Description
S1	Pumping increases $1.4 \times 10^7 \text{ m}^3/\text{yr}$	A	Private bottle water supply
S2	Pumping remains constant	B	Centralized water treatment – 0% subsidy
S3	Pumping decreases $0.4 \times 10^7 \text{ m}^3/\text{yr}$	C	Centralized water treatment – 100% subsidy

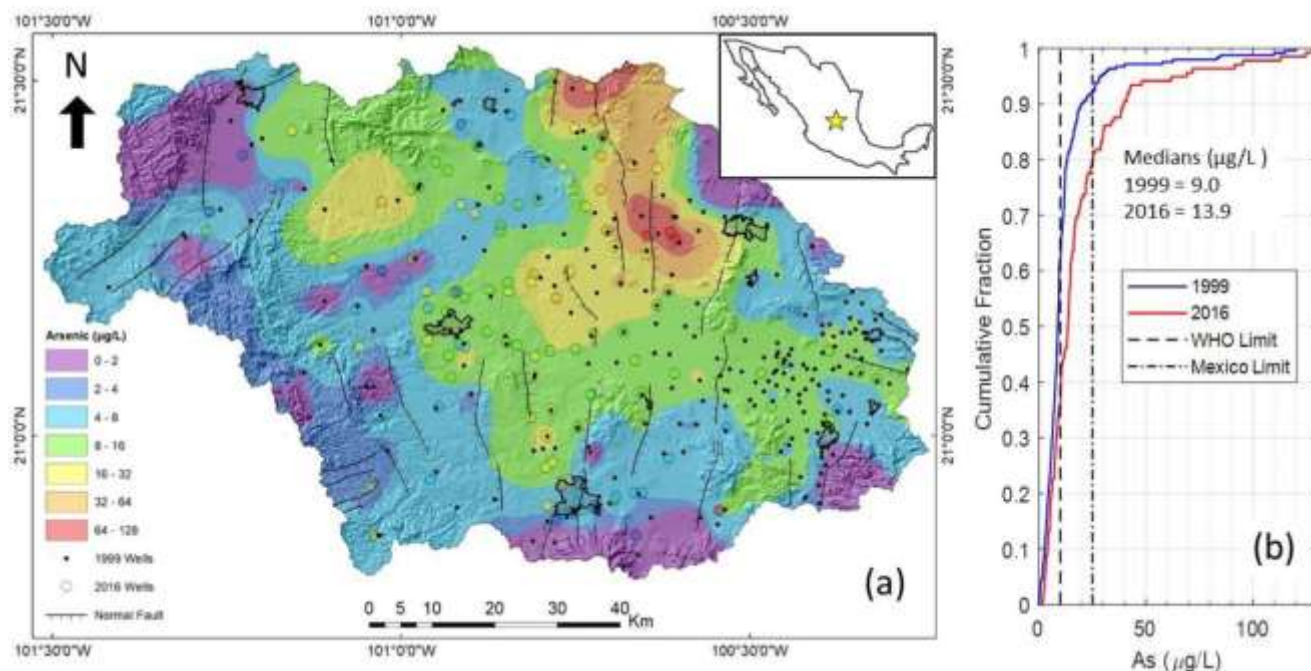


Figure 2. (a) Arsenic concentrations in 137 wells sampled in 2016 in the independence Basin (large colored circles) overlain on contoured concentrations of 246 wells sampled in 1999 (black circles). The locations of major faults are noted. Urban areas are indicated with cross-hatching. (b) Cumulative histogram of As concentrations in 1999 (blue) and 2016 (red). Arsenic drinking water limits of WHO and Mexican Government indicated by black vertical dashed lines.

2.2. Study Area

2.2.1. Physiography, Geology, and Hydrology

The Upper Rio Laja River watershed is also known as the Independence Basin (Ortega-Guerrero, 2009) (Figure 2; Figure S1 in Supporting Information S1). It is encircled and underlain by mountain ranges composed of volcanic rock and extinct volcanoes. The total relief of the basin ranges from 1,900 to 3,000 masl. The upper several hundred meters of the relatively flat central part of the basin is composed of poorly consolidated sandstone and conglomerate eroded from the surrounding mountains. Numerous normal faults create grabens and half grabens, which are infilled with sediment (Castro et al., 2021; Del Pilar-Martinez et al., 2020; Del Rio et al., 2020). This basin is typical of other semi-closed basins throughout the Central Highlands of Mexico (Del Rio et al., 2020; Loza-Aguirre et al., 2012). The low-lying, middle area of the basin is intensively irrigated with groundwater for growing crops.

The basin has only one outlet, which is regulated at the Ignacio Allende Dam. The Ignacio Allende reservoir is adjacent to the largest and fastest growing city in the basin, San Miguel de Allende. The basin has a surface area of approximately $6.84 \times 10^9 \text{ m}^2$ (6,840 km²) and receives 580 mm of rainfall annually (Mahlknecht et al., 2004). The National Commission for Water (CONAGUA) jointly manages the surface and groundwater resources in this basin by dividing the basin into four administrative aquifer zones. These are the Cuenca Alta del Rio Laja, Dr. Mora y San Jose Iturbide, Laguna Seca (LS), and San Miguel de Allende (Figure S1 in Supporting Information S1).

2.2.2. Population, Employment, Economy, and Politics

Approximately 744,000 people live in the basin spanning seven municipalities: San Miguel de Allende, Dolores Hidalgo, San Luis de la Paz, San Diego de la Union, Doctor Mora, San Jose Iturbide, and San Felipe (INEGI, 2021). Agriculture in the state of Guanajuato accounts for approximately 4.6% of economic output and employs 13% of the working population.

Table 2
Descriptions of Equations Used in the Systems Model

Process name	Equation	#
Hydrologic Cycle	$AA = EEEE + II + RR$	1
Vertical Recharge—water budget method	$AA_{vv} = QQ_{tt} + (HH_{tt-1} - HH_{tt})SS_{yy} - QQ_h$	2
Recharge—chloride mass balance method (Clark & Fritz, 1997)	$AA = \frac{cccc}{precip} PP$	3
Annual groundwater deficit	$AA_{tt} = QQ_{tt} - II$	4
Lift Height as a function of groundwater deficit	$AA_{tt} = AA_{oo} - \frac{DD}{SS_{yy}AA}$	5
Energy consumed by irrigation pumping (Scott, 2011)	$AA_{tt} = 438 + \frac{ee}{PP}$	6
Total dynamic head for pumping groundwater (extended Bernoulli equation) (Weiner & Matthews, 2003)	$ATT_{tt} = \frac{vv2}{2gg} + \frac{dd}{yy} + HH_{tt} - A_{LL}$	7
Price of energy for pumping groundwater for a given sector with subsidization rate S_E (Scott, 2011)	$AAEE_{tt} = RREEE_{tt}(1 - SSEE)$	8
Total cost for drilling new wells to reach water table during year t	$AA_{well_{tt}} = (HH_{tt} + ZZ_{oo}) \left(\frac{dd_{tt}}{\Delta AA} \right) \left(\frac{qq}{pop_{well}} + \frac{qq}{ag_{tt}} \right)$	9
Crop mass produced per volume of water (Hoekstra et al., 2011)	$AA_{tt} = \frac{QQ}{SS}$	10
Concentration of contaminant AA at depth	$AA_{iii} = kk_{iii}$	11
Concentration of contaminant AA with mixing in a long-screen well	$AA_{iii_{well}} = \frac{kk_{HH}}{tt + kk_{iizz}}$	12
IQ point decrement as function of childhood exposure to concentrations of contaminant AA in drinking water (Wasserman et al., 2004)	$IQ_{decr, tt} = III_{oo} - \beta\beta_{ii} (\log_{ee} CC_{ii, tt})$	13
Personal income at time t	$\ln_{pppppp} = \ln_{ppppppoo} (1 + kk_{III})_{pp}$	14
Fractional reduction of personal income as function of IQ decrements (Grosse et al., 2002)	$\frac{(\Delta III)}{III} = \frac{III}{III_{tt} \Delta III} (IQ_{decr, tt})$	15
Reduced personal incomes from IQ decrements (Attina & Trasande, 2013)	$\ln_{pppppp} = \ln_{ppppppoo} (1 + kk_{III})_{pp} (1 - \Delta \ln)$	16
Personal income subtracting cost of mitigation	$\ln_{pppppp} = \ln_{ppppppoo} (1 + kk_{III})_{pp} - TT (CC_{ii})$	17
Population growth rate	$POP_{tt} = POP_{oo} e^{kk_{pop, tt}}$	18

2.3. Components of the Model

Mathematical equations that describe each process included in the model are described in Table 2 and the meaning and values of each parameter are in Table 3. In the following sections, the empirical data and theory used to constrain model subprocesses are described for this study area.

2.3.1. Hydrologic Cycle

Between 1980 and the present, the water tables have fallen at an average rate of 1.65 m/year (Figure S2 in Supporting Information S1) (Li et al., 2020). New wells must be drilled to reach the falling water table. Thus over the period from 1975 through 2012, well depths deepened at approximately the same rate water tables fell (Figure S3b in Supporting Information S1). The median standing water height in the wells is 100 m (z_w), which is the distance below the water table (H) (Knappett et al., 2018).

The average rate of water table decline across the basin depends on the rate of recharge (I), the rate of pumping (Q), and specific yield (S_y) of the aquifer. The hydrologic cycle equation (Equation 1 in Table 2) describes the water budget for this basin. The annual volume of rain falling on the basin (P) was approximated by multiplying the area of the basin with the average annual rainfall (580 mm) (Mahlknecht et al., 2004) (Figures S4 and S5 in Supporting Information S1). This is equal to 4.56×10^9 m³/year. On average, only 6.7×10^6 m³/year flowed out of the basin (R) over the Ignacio Allende Dam during the period from 2005 through 2013 (unpublished data from CONAGUA). The remaining water exits the basin as evaporation and transpiration (ET) or infiltrates (I) to recharge the aquifer.

Recharge estimates were drawn from studies that used two different techniques, namely vertical recharge (Equation 2 in Table 2) and the chloride mass balance approach (Equation 3 in Table 2). The vertical recharge method multiplies the annual change in water table elevation by S_y and subtracts the water volume that entered the aquifer

Table 3
Parameters and Initial Conditions Used in Systems Model

Variable	Variable description	Units	Initial, Fixed or Fitted value (range of likely values)
<i>Hydrogeology and geochemistry</i>			
AA	Area of basin	[m ²]	6.84×10^9
AA	Annual basin-wide precipitation ($P = A \times$ average annual rainfall 580 mm (500–610)) (Figure S5 in Supporting Information S1)	[m ³]	3.98×10^9 (3.42^{25} , $4.17^{75} \times 10^9$)
I/PP	Fraction of P that Recharges aquifer (Mahlknecht et al., 2004)	[-]	0.052 (0.04 ^L , 0.073 ^H)
AA	Annual basin-wide aquifer recharge	[m ³]	2.07×10^8 (1.59 , 2.91×10^8)
AA_{rv}	Vertical recharge occurring directly to a defined area of an aquifer	[m ³]	
$AAAA$	Annual evapotranspiration	[m ³]	3.77×10^9 (3.69 , 3.82×10^9)
AA	Annual basin-wide runoff	[m ³]	6.77×10^7
AA_h	Horizontal flow into a defined area of an aquifer	[m ³]	
AA_{tt}	Annual basin-wide pumped groundwater for all sectors	[m ³]	
$AAAA_{aoo}$	Basin-wide pumped groundwater for agriculture in 2020 (CONAGUA, 2020e)	[m ³]	4.63×10^8
AA_{resoo}	Basin-wide pumped groundwater for residential use in 2020 (CONAGUA, 2020e)	[m ³]	4.52×10^7
	Chloride concentration in rainfall	[—mgL]	0.16
$AAAA_{precip.}$			
$AAAA_{gw}$	Chloride concentration in well water	[—mgL]	
AA_{tt}	Lift height from water table to surface	[m]	$H_o = 100$ (70^{25} , 150^{75})
AA_{tt}	Annual basin-wide groundwater recharge deficit	[m ³]	
ALL	Dynamic head loss owing to friction	[m]	
AA_{yy}	Specific Yield (CONAGUA, 2020a, 2020b, 2020c, 2020d; Consultores en Geologia, S. A. d. C. V., 1992)	[-]	0.04 (0.03, 0.05)

AA	Depth below ground surface	[m]	
AA_{oo}	Length of wells below water table	[m]	$z_o = 100$ (49 ²⁵ , 163 ⁷⁵)
A_{TTt}	Total dynamic head	[m]	
AA_{iiii}	Median contaminant concentration in wells at time t	[μg] or [mg]	13.9 (As), 0.99 (F) (2020), 9.7 (As), 0.70 (F) (1999)
AA_{ii}	Linear rate of increase of contaminant AA concentration with depth in aquifer z	[$-\mu\text{g}/\text{m}$]	0.0953 (0.0927 ^{LB} , 0.0979 ^{UB}) (As), 0.0072 (0.0056 ^{LB} , 0.0088 ^{UB}) (F)
<i>Public health and human development</i>			
$AAAA_{tt}$	Median population IQ at time t	[1 : 100]	
$AAAA_{oo}$	Default IQ		100
AA_{ii}	IQ point decrements per $\log_{ee}[\frac{CC}{iiii}]$ (Rocha-Amador et al., 2007; Wasserman et al., 2004)		-1.65 (-1.24, -2.06) (As), -10.1 (-7.6, -13.9) (F)
(ΔIII)	Fractional suppression of income per IQ decrement (Grosse et al., 2002)	[IQpoint ⁻¹]	0.02 (0.015, 0.025)
<i>Economics</i>			
$In_{p,t}$	Per capita income at time t	[USD]	
$In_{p,o}$	Median 2020 per capita income in rural Guanajuato (also poverty line)	[USD]	1,165
$In_{p,mit}$	Expected per capita income after drinking water quality mitigation	[USD]	
LE	Life expectancy in Guanajuato (2020)	[yr]	76
AA_n	Personal income growth rate	[yr ⁻¹]	$\frac{1}{}$
AA_{pop}	Population growth rate	[yr ⁻¹]	0.01
POP _o	Initial population of basin in 2020	[people]	744,000

Table 3 Continued

Variable	Variable description	Units	Initial, Fixed or Fitted value (range of likely values)
pop _{well}	Number of people utilizing each municipal supply well	[people _{well}]	710 ²⁵ , 1,250 ⁵⁰ , 1,600 ⁷⁵ , 10,000 (San Miguel de Allende)
AA_{well}	Median annual pumped volume for irrigation wells in the basin	[m _{yr} ³]	95,000 ⁵⁰
$\Delta \frac{PP}{\Delta_{well}}_{zz}$	New water production well drilling and installation cost per meter	[USD _m]	293
AA_{EEtt}	Price of electricity to irrigate crops	[USD]	
$T(C_i)$	Water treatment cost for contaminant AA	[person-yr USD]	127 (Bottled), 18 (Centralized RO)
$AA_{crop,ii}$	Market price for crop i (SIAP, 2020)	[tonne ^{USD}]	182 ^{vw} , 243 ²⁵ , 434 ⁵⁰ , 737 ⁷⁵ , 448 (broccoli)
AA	Water use efficiency (Mekonnen & Hoekstra, 2011, 2013)	[tonne ^{m3}]	1,549 ^{vw} , 326 ²⁵ , 477 ⁵⁰ , 1,538 ⁷⁵ , 296 (broccoli)
AA_{EF}	Unsubsidized energy rate or tariff (SENER, 2018)	[USD _{kwh}]	0.017
$AA_{oB,tt}$	Energy consumed for irrigation pumping	[kwh]	

$AA_{dom,zz}$	Energy consumed for domestic pumping	[kwh]	
AA_{EE}	Electricity subsidy (SENER, 2018)	[-]	0.88 (agriculture), 0.65 (residential)
AA	Unit conversion term (Scott, 2011)	[-]	0.0026
AA	Electromechanical pump efficiency (Scott, 2011)	[-]	0.52
AA	Specific weight of water	[ft ⁻³]	62.4

Note. ^{L,H}Low and High ends of observed range. ^{LB,UB}Lower and Upper Bounds of 95% Confidence Interval of fitted term. ^{vw}Volume-weighted average. ^{25,50,75}Percentiles of observed distribution of values.

laterally by applying Darcy's Law to the observed hydraulic gradients and known transmissivity (T) of the aquifer (Equation 2 in Table 2). When this approach was applied on the four administrative aquifers comprising this basin, the total recharge in 2020 was calculated to be $3.35 \times 10^8 \text{ m}^3/\text{yr}$ (CONAGUA, 2020a, 2020b, 2020c, 2020d) or 7.3% of total precipitation falling on the basin (Table 3). In contrast, the chloride mass balance approach (Clark & Fritz, 1997) assumes that the enrichment in chloride concentrations observed in groundwater (cl_{gw}) over rainfall (cl_{precip}) is caused by ET (Equation 3 in Table 2). Using this technique, one study estimated basin-wide average recharge to be $1.98 \times 10^8 \text{ m}^3/\text{yr}$ (4.3% of P) (Mahlknecht et al., 2004). An independent analysis utilizing a more recent data set and excluding samples that appeared to be contaminated by chloride from geothermal sources based on the Cl:Br mass ratios (Alcala & Custodio, 2008; Knappett et al., 2018) found recharge to be $1.82 \times 10^8 \text{ m}^3/\text{yr}$ (4.0% of P). The average of these three independent estimates was utilized in the model (5.2% of P) (Table 3).

In 2020 the median depth to the water table was 100 m (H_o) with 25th and 75th percentile depths of 70 and 150 m, respectively (Li et al., 2020). Combined pumping rates (Q_i) across the basin for agriculture (Q_{oag}) and domestic (residential) (Q_{ores}) purposes in 2020 were obtained from CONAGUA (Table 3) (CONAGUA, 2020e) and used to calculate the water deficit (D_i) (Equation 4 in Table 2). This deficit translates to an increase in lift height of 0.59 m/yr (Equation 5 in Table 2) if the reported pumping was evenly distributed across the entire basin. This calculation is impacted by three sources of bias. First, pumping is not distributed evenly but rather, is concentrated on the low-lying central part of the basin; so greater drawdown would be expected in the parts of the basin being pumped. Second, a range of S_y values have been reported across the basin but only a limited number of measurements are available (CONAGUA, 2020a, 2020b, 2020c, 2020d; Consultores en Geologia, S. A. d. C. V., 1992; Ingenieros Civiles y Geologos Asociados, S. A., 1980). Third, the reported combined pumping rate does not account for pumping from unregistered wells, which are abundant, nor does it consider that farmers routinely pump more than their permitted volumes. In spite of these limitations, this water budget and the 2020 official pumping rates were used for the starting year of the model.

2.3.2. Energy Consumed by Irrigation Pumping

As the water table falls, more energy must be consumed to lift the water to the surface. The energy consumed (E_i) varies with pump efficiency (e), lift height (H_i), and pumping rate (Q_i) (Scott, 2011) (Equation 6 in Table 2). When lift height exceeds 50 m, it dominates the calculation of total dynamic head (h_T) (Equation 7 in Table 2), since the kinetic energy and friction loss (h_L) terms are negligible (Weiner & Matthews, 2003).

In this basin, most pumped groundwater (>80%) is used for irrigation of mostly agro-export crops. Therefore, outside investors and international market prices drive the majority of the irrigation pumping. The main cost increase is from drilling and lifting water to the surface. The state blunts the impact of rising electricity costs to irrigators by raising subsidies for farmers (Hoogesteger & Wester, 2017; Scott, 2011). Similarly, the state subsidizes the majority of the costs of constructing new community wells for domestic (municipal) supply.

The price of energy (P_E) depends on the energy tariff (R_E) and the rate of subsidization (S_E), which is currently about 88% for the agriculture sector (SENER, 2018) (Equation 8 in Table 2). The nighttime pumping rate that farmers pay for irrigation is 0.02 USD/kWh (Scott, 2011), which has been stable over the last two decades (Hoogesteger & Wester, 2017; SENNER, 2018). In 2018, the subsidized residential tariff for electricity in Mexico was approximately 0.06 USD/kWh (SENER, 2018). For comparison, in 2018, the industrial, services, and commercial sectors paid 0.08, 0.13, and 0.16 USD/kWh, respectively (SENER, 2018). Unlike residential and agriculture users, the tariffs for these sectors have been rising steadily over the past two decades. To confirm which tariff the communities in the basin pay for pumping their residential water supply, we compared the reported monthly electricity bills for 19 wells to the lift energy (Equation 6 in Table 2) based on the depth to water and the annual pumped volumes. This resulted in a median tariff of 0.16 USD/kWh, which suggests that communities pay the services tariff to pump their wells.

2.3.3. Cost of New Well Installation With Falling Water Tables

Falling water tables force well owners to deepen their wells or drill new ones. The cost of a 550 m deep well in the 137 well database that was collected in the field was installed in a community in the LS administrative zone in the eastern part of the basin. Here the water table is 150 m below the ground surface. The well was publicly reported to cost 161,200 USD, fully installed. The community provided 10% of the cost, and the state and federal governments paid 10% and 80%, respectively. Although this very deep well has a 14 inch outer casing diameter, it is only set to pump at a rate of 6.5 L/s. This pumping rate is on the low end for this basin. Pumping rates of urban supply wells commonly range from 30 to 100 L/s, but much lower pumping rates are typical for small communities that require smaller volumes of water (see Figure 5 in Knappett et al., 2020). This well replaced a previous well that was 170 m deep and was installed in 1985 and had since gone dry. This cost of the new well installation is approximately 293 USD/m (Table 3). Other new wells in the region had a similar cost per meter of completed production well. For comparison, this amount is approximately one third of the cost per m of installing a fully fitted 300 m water well for irrigation in the Central Valley, California (1,083 USD/m) (Howard, 2014). The upper geologic material in each basin is poorly consolidated sedimentary rock and therefore similar in terms of difficulty drilling. Detailed analyses of the drill cuttings from the LS well (Shepherd, 2018), surface geology map, and other reported borehole lithologies throughout the basin (Figures S6 and S7 in Supporting Information S1) (Figure 2 in Knappett et al. (2020)) suggest, however, that the unconsolidated sediment in the LS aquifer transitions to volcanic rock at 300 m depth. Thus, this number represents an average cost of drilling through sedimentary and volcanic rock.

The annual cost of new well drilling as a function of the falling water table (H_t) was calculated using Equation 9 (Table 2). This calculates the annual basin-wide price of new well drilling ($P_{well,t}$). This equation calculates the forced new well depths ($H_t + z_o$) multiplied by the cost per m of the installed well to obtain the cost of a new well installed that year. This cost is then amortized over the lifetime of the well, which is calculated by the instantaneous rate of water table decline (dH_t/dt) divided by z_o . The number of municipal wells that are in operation each year, and therefore vulnerable to falling water tables, is calculated by the basin population (POP_t) divided by the median population served by each well (pop_{well}). Similarly, the number of irrigation wells are calculated by the current irrigation pumping rate (Q_{agt}) divided by the median annual pumped volume of an irrigation well in 2016 (q_{well}) (Table 3).

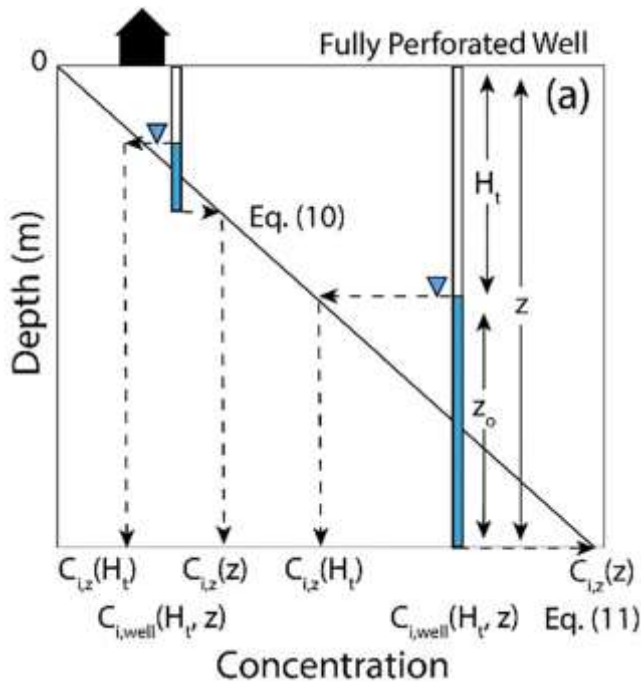


Figure 3. Modeling increasing As and F concentrations as a function of both well depth (z) and depth to water table (H_t). The black line represents the concentration of a geogenic contaminant i that increases linearly with depth within the aquifer. Concentration at the water table and bottom of a fully perforated well is equal to $C_{i,z}(H_t)$ and $C_{i,z}(z)$, respectively. The average of these is $C_{i,well}(H_t, z)$ (Equation 11 in Table 2) is the mixed concentration of contaminant i in the aquifer from the water table (H_t) to the well bottom (z).

2.3.4. Crop Mass Produced and Revenue Generated per Volume of Water

If only irrigated crops are considered across the basin (excluding crops that were watered only with rainfall), approximately $1.0 \times 10^9 \text{ m}^3$ of water was used for growing crops in 2020 (Table S1 in Supporting Information S1). This volume was calculated by multiplying the reported mass of crop grown (SIAP, 2020) by the average water footprint for each crop (Equation 10 in Table 2; Mekonnen & Hoekstra, 2011). This amount includes rain water, of which approximately $3.3 \times 10^8 \text{ m}^3$ fell on the reported area of irrigated lands. Rainwater, however, would be used less efficiently by crops compared to applied irrigation water, owing to the timing of the rainfall events and the rainy season (May–August) not coinciding with crop growth periods. The water consumed by crops on irrigated lands minus this rainfall amount ($6.7 \times 10^8 \text{ m}^3$) approximately matches the independently reported permitted irrigation pumping across the basin of $4.63 \times 10^8 \text{ m}^3$ (Table 3) (CONAGUA, 2020e). Based on their average water footprints (Mekonnen & Hoekstra, 2011, 2013), reported crop mass grown (SIAP, 2020), and Equation 10 in Table 2, the eight crops that consumed the most water on irrigated lands only were Oats (39%), alfalfa (33), corn (12), beans (4), broccoli (4), asparagus (2), green chiles (2), and tomatoes (1).

The revenue generated per water volume consumed to grow a certain crop (USD/ m^3) is calculated by dividing the crop price (P_{crop}) by the average water footprint (s). This was highly variable across the eight crops that consumed the most water (Table S1 in Supporting Information S1). The largest and smallest values per water volumes were green chile (2.01 USD/ m^3) and oats 0.01 USD/ m^3 , respectively (Figure S8b in Supporting Information S1). The volume-weighted average for crops grown on irrigated lands in 2020 was only 0.12 USD/ m^3 . A high value and low-water footprint crop that is likely to be representative of the agricultural sector of the future is broccoli. In

2020, broccoli sold for 448 USD/tonne and requires approximately 296 m^3 /tonne of water (Fulton et al., 2019; Mekonnen & Hoekstra, 2011). Thus, the revenue generated from the sale of broccoli per water volume is 1.51 USD/ m^3 .

Agricultural production should respond to changing prices and costs. In particular, as the water table falls and pumping heights increase, costs rise, which theoretically would put downward pressure on agricultural production, even if farmers are shielded from most of these costs through government subsidies. On the other hand, increasing populations and standards of living would tend to push agricultural demand up. Since it is impossible to know if the downward or upward pressures will prevail, in our scenarios, we assumed that agricultural production is a linear function of the amount of water pumped for irrigation, which is the flow that is varied exogenously in the simulations.

2.3.5. As and F Concentrations as Function of Depth to Water Table and Well Depth

To link water table declines to groundwater quality it is important to constrain the subsurface flow, transport, and chemical reaction processes. In this basin, the most likely causes of groundwater quality deterioration is tapping older, hotter, and more mineralized groundwater from shallow geothermal heat. The specific geochemical reactions are detailed in previous studies from this and other analogous basins (Knappett et al., 2020; Morales-Arredondo et al., 2018; Rango et al., 2013; Xing et al., 2022). To obtain typical basin-wide future As and F concentrations as a function of depth to the water table (H_t), observed concentrations in long-screened wells with known depths ($n = 106$) across the basin were fit to a linear equation of a plane that takes into account the volumetric mixing that occurs across the standing water height within continuously screened wells (Equation 11 in Table 2; Izbicki et al., 2015; Mayo, 2010) (Figure 3). In this model, a linear increase in As and F concentrations

at depth (Equation 10 in Table 2) underlies the mixing model. The mixing model calculates the average concentration at the depth of the water table and the depth of the bottom of the well ($H_t + z_o = z$). Future well depths were calculated using future lift heights (H_t) plus z_o . This model makes predictions of both past and future As and F concentrations as a function of H_t and z . To test this model, it must not only explain the spatial distribution of As and F in 2016 but also the temporal distribution over a period when the water table was observed to fall. The successful test against historical As and F concentrations in 1999, when the water table was higher, is presented in Supporting Information S1.

Observed As and F concentrations were fit to Equation 11 in Table 2 within 57 wells across the basin for which H_t and z were known (Figures S9 and S10 in Supporting Information S1). This yielded k_{As} and k_F values of 0.0953 and 0.0072 (mg/L/m), respectively. Using the same approach as for As and F, the vertical geothermal (k_{Temp}) gradient underlying the central part of the basin was found to be $2.0 (\pm 0.5)^\circ\text{C}/100\text{ m}$ (Figure S11 in Supporting Information S1). This is lower than the typical $8^\circ\text{C}/100\text{ m}$ geothermal gradient found throughout the Trans-Mexican Volcanic Belt just south of this basin (Prol-Ledesma & Moran-Zenteno, 2019).

2.3.6. IQ Suppression as Function of As and F Concentrations in Drinking Water

This study focusses on the neurotoxic effect of As and F in child cognitive development as an example of one health and economic impact from exposure. The thresholds at which negative health effects occur and the shape of the dose-response curve for a given neurotoxin are uncertain. A general feature, however, of some well constrained dose-response curves of inorganic neurotoxins (i.e., lead (Pb)) is their inverse shapes (Grandjean & Landrigan, 2006). In such cases, the steepest IQ reductions occur across the low concentration end of the exposure scale (Grosse et al., 2002).

The neurotoxic effects of As ingestion by children are significant even at low concentrations. But the empirically measured dose-response relationship between chronic exposure to As in drinking water or diet and some measurement of cognitive performance ranges considerably (Desai et al., 2020; Grandjean & Landrigan, 2006; Hamadani et al., 2011; Nahar et al., 2014; Rocha-Amador et al., 2007; Rodriguez-Barranco et al., 2013; Signes-Pastor et al., 2019; Vahter et al., 2020; Wasserman et al., 2004, 2014, 2016). The reasons for this variability include (a) different cultural setting and age of children to whom a given intelligence test was applied (WISC-III, WISC-IV, Cambridge Neuropsychological Test Automated Battery, and McCarthy Scales of Children's Abilities); (b) the chemical form of As ingested; (c) genetic and/or metabolic differences across individuals and groups in their ability to detoxify As; (d) whether drinking water or another biological sample (urine, blood, hair, or toenails) was taken to assess exposure and the specific biochemical form of As measured (MMA, DMA, and total); and (e) other study design factors such as sample size and specific confounding variables included in the model (i.e., mother's education, household income, quality of home environment, and co-exposure to lead or manganese). In spite of these differences, all studies conclude that As exposure, even at levels near the WHO guideline, have a clear negative impact on child IQ. Longitudinal studies suggest that the effect is irreversible (Vahter et al., 2020; Wasserman et al., 2016).

The observed threshold of a neurotoxic effect from As exposure ranges across studies. This threshold can be estimated by studies that regressed a measure of cognitive performance on quintiles of As exposure levels. For example, in a cross-sectional study with 272 9–10 year old school children in Maine, USA, children drinking private well water with As concentrations exceeding $5\text{ }\mu\text{g/L}$ had approximately 6.1 lower IQ points than children drinking less than this amount (Wasserman et al., 2014) (dashed line, Figure 4a). In a longitudinal study with 1,523 10 year old children in MATLAB, Bangladesh, a large decrease (7.2) in the Full Development Score in the WISC-IV test (modified for 10 year old Bangladeshi children) was observed when total urinary As concentrations exceeded approximately $30\text{ }\mu\text{g/L}$ (Vahter et al., 2020). The difference in the thresholds may be partly owed to the exposure levels being much lower in the Maine study than those in the Bangladesh study; however, the magnitude of the effects are similar in both cases.

Other studies had the statistical power to constrain a continuous dose-response relationship where As concentrations in water or urine are \log_e -transformed and regressed upon IQ or raw scale point decrements (Equation 13 in Table 2) while controlling for confounding variables. A cross-sectional study with 201 10-year-old children in Araihaazar, Bangladesh, found that the regression coefficient, β_{As} , was approximately -1.65 when $\log_e(\text{As})$ concentrations in drinking water were regressed upon Full-Scale raw scores (Wasserman et al., 2004).

A longitudinal study with 1,700 5 year olds in MATLAB, Bangladesh, observed a β_{As} of -1.4 only for girls when $\log_e(As)$ concentration in urine were regressed upon Full-Scale IQ scores corrected for age (Hamadani et al., 2011). In spite of the fact that it only applies to full-scale raw scores, the β_{As} value of -1.65 was chosen for the model to approximate the reduction in IQ points because this model was continuous and regressed on As concentrations

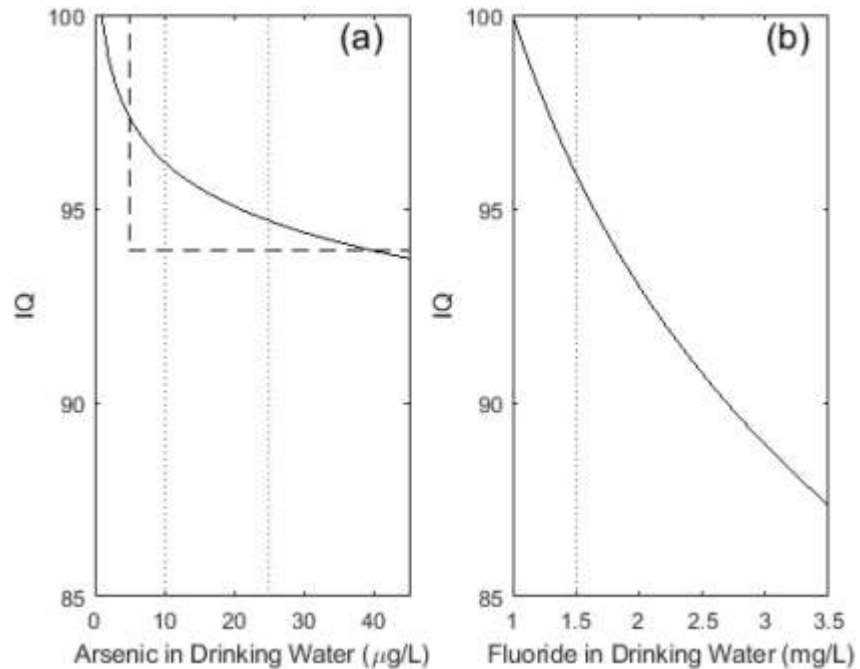


Figure 4. Published dose-response curves of IQ reduction owing to exposure to As and F in drinking water. (a) Continuous and step style dose-response curves (Wasserman et al., 2004, 2014). (b) Study by Rocha-Amador (2007). Vertical blue and red dotted lines represent the WHO and Mexican drinking water limits, respectively.

in drinking water (solid line, Figure 4a), and the magnitude of the effect is very similar to several high quality studies reviewed above.

A neurotoxic effect of exposure to F in drinking water has been widely reported (Choi et al., 2012). Many of these epidemiologic studies, however, did not control for a wide range of potentially confounding variables. Nevertheless, a pooled meta-analysis on 27 studies reported a 0.44 standard deviation shift to the left owing to “exposure” to high F (Choi et al., 2012). This corresponds to approximately seven IQ points on a normally distributed intelligence curve (Choi et al., 2015). The exposed group was typically exposed to F concentrations ranging from 1 to 4 mg/L but ranged up to 11 mg/L in several studies.

To the authors' knowledge, only one study has published a continuous dose-response curve for exposure to F in drinking water that controlled for confounding variables. This cross-sectional study with 155 children from 6 to 10 years old was conducted 100 km north of our study basin in San Luis Potosi (Rocha-Amador et al., 2007). Fluoride concentrations in that study spanned a similar range to those in our study basin (<0.5–16 mg/L). The current median F concentration in our study area is approximately 1 mg/L (Knappett et al., 2020). Based on the reported value of β_F of -10.1 (units of $\log_e(\text{mg/L})$), no reduction in IQ is predicted based on the current median concentration. However, this coefficient suggests that consuming water at the WHO limit of 1.5 mg/L may lower IQ by four points (Figure 4b). This large effect is supported by a recently published longitudinal study that was performed in Mexico City with 299 mother-child pairs. The authors found that each increase of 1 mg/L increase in creatinine-adjusted F concentration in maternal urine over a threshold of 0.8 mg/L during gestation was associated with five IQ point reductions in their 6–12 year old children (Bashash et al., 2017). The range of maternal, creatinine-adjusted F concentration in urine was 0.23–2.14 mg/L. Thus, although the question of whether exposure to F concentrations less than 4 mg/L in drinking water has neurotoxic effects is debated in the

literature, a large body of formal peer-reviewed evidence suggests that it can negatively impact cognitive development during certain windows of susceptibility (Till & Green, 2021). What is even less understood is how geogenic neurotoxins collectively impact cognitive development. In this study, we assume the effects are independent and can be simply added.

2.3.7. Efficacy and Costs of Paying for Drinking Water Quality Mitigation

2.3.7.1. Self-Supply With Bottled Water

Although bottled water is not economical compared to piped water solutions and centralized treatment, it is nonetheless widely relied upon for drinking and cooking water. Mexico in particular is considered to be the bottled water capital of the world (Green, 2018). Past studies on a limited scale in Mexico have found unacceptably high concentrations of these dissolved elements in bottled water (Del Razo et al., 2018). A large-scale study in Italy found widespread low levels of geogenic contaminants in bottled water, which, in a few cases, exceeded the WHO standards (Cidu et al., 2011). Therefore, geogenic contaminants that are widely present in a region will also likely be found in bottled water and this may contribute to the overall exposure levels. Households commonly continue to be exposed to As and F in their tap water even while using bottled water. A governmental intervention in central Mexico (San Luis Potosi) to reduce human exposure to F in piped water subsidized the costs of bottled water but found that exposure measured in urine samples remained high because people continued to prepare their food with tap water (Del Razo et al., 2018). The typical cost to a household of paying for bottled water for both drinking and cooking is 634 USD/yr for a household of five people, or 127 USD/person/yr. Over the 100 years simulation period, the cost of bottled water was assumed to be constant in 2020 dollars and this water was assumed to contain low concentrations of As and F ($<1 \mu\text{g/L}$ and $<1 \text{mg/L}$, respectively).

2.3.7.2. Centralized Community Water Treatment

Reverse osmosis (RO) is the most widely used treatment method in Mexico for As and F at the community and household scales (Del Razo et al., 2018). More generally, it is also the most widely used technology for removing unwanted inorganic ions in water (Boden & Subban, 2018). This widespread use of RO poses a health risk to people consuming too little dissolved geogenic elements such as F and lithium (Li), which are necessary for a healthy diet (Sedlak, 2019). The micronutrient deficient water can be remineralized with salts after passing through the RO system; however, this additional step is typically omitted. The state and federal governments have sponsored mitigation on an ad-hoc basis in the past when particularly high concentrations of As and F were found in well water, but there is no blanket testing and no uniform concentration threshold above which public funds are provided for treatment for As and F across Mexico (Del Razo et al., 2018). We compare the costs and benefits to households and taxpayers if centralized treatment is 100% funded by federal and state governments. This has been done for chlorination as a treatment method at nearly all drinking water sources since 1991 (Del Razo et al., 2018).

A report from the non-governmental organization Oxfam summarized the current costs of constructing and operating small-scale community RO plants in developing countries (Boden & Subban, 2018). The actual costs of building and operating an RO plant depend on the costs of parts, expertise, labor, energy, and the method of disposal of the brine waters (US EPA, 2019). A full analysis of these are beyond the scope of the present study and the costs presented herein are only estimates. For performing RO on low-salinity waters (e.g., groundwater in the study basin), approximately 1kWh/m^3 is needed. An additional 1kWh/m^3 is required for cleaning and distributing the water through the community and disposing of the leftover brine (Boden & Subban, 2018). Therefore, 2kWh/m^3 is implemented in the model for the energy consumption for RO treatment. At the average 2018 services electricity tariff of 0.13USD/kWh (SENER, 2018), this corresponds to a cost of 0.26USD/m^3 .

For mild climates as in Guanajuato, low- and middle-class household water consumption is reported to be approximately 100 and 195 L/person/day (CONAGUA, 2007; Cruz et al., 2017). Thus, the average of 147.5 L/person/day was implemented. For a community supplied tap water by a typical small-scale RO treatment operation, this would translate to $54 \text{m}^3/\text{person/yr}$ and 9.7 USD/person/yr for electricity. For community-scale RO filters, energy will comprise over 50% of the operating costs (Boden & Subban, 2018). The capital costs of installing an RO system that would provide a community with $10 \text{m}^3/\text{day}$ range from 4,000 to 8,000 USD. This

would supply 68 people with drinking water. We assumed the mid-range capital cost (6,000 USD) and amortized this cost over 10 years, which translates to an additional cost of 8.85 USD/person/yr. Therefore, the total cost per person for a community RO system, excluding the cost of labor, was assumed to be approximately 18.55 USD/person/yr. Although it is only an estimate, this is a fraction of the cost of bottled water, which only supplies water for drinking and cooking, not for all household needs as centralized treatment provides. Furthermore, the cost of centralized treatment options, such as RO, are likely to continue to decrease in the future.

2.4. Model Implementation

All governing equations are expressed in their analytical or finite forms (Table 2). The system of equations was solved in MATLAB (version R2019a). The simulation was run at 1 year timesteps for a period of 100 years. Initial conditions and model parameters were classified as either initial, fixed, or fitted (Table 3). The fitted parameters included average coefficients from dose-response studies for human exposure to As and F concentrations and rates of increase in As and F concentrations with well depth (Section 3.2). Key outputs of the simulation were change in lift heights, energy consumption and cost, As and F concentrations over time, mean childhood IQ reductions, and the impacts of these IQ reductions on mean personal earnings. Driving the forward model are the three different future pumping rate scenarios that were previously described and are detailed in Table 1.

3. Results and Discussion

3.1. Long-Term Water Level Declines and Energy Demand for Irrigation

Pumping rates in year one (2020) were set as the summed volume of concessions for registered wells (CONAGUA, 2020e). After that, the three pumping rate change scenarios were implemented (Figure 5a). Under S1, the lift height would reach 426 m in 2120 (Figure 5b), and total annual energy demanded for irrigation pumping would reach 3,918 GWh (Figure 5d). Given that 1,737 kWh powers a Mexican home for 1 year (Oropeza-Perez & Petzold-Rodriguez, 2018), this is equivalent to 2.56 million homes. In contrast, energy demanded for irrigation pumping would reach 481 and 72 GWh for the static (S2) and decreasing (S3) pumping rate scenarios, respectively.

3.2. Childhood IQ and Income for Population Living in the Basin

Irrigation pumping will continue to force communities to install deeper wells in the coming decades. A 2% reduction in lifetime earnings per IQ point decrement was determined (Attina & Trasande, 2013; Grosse et al., 2002). Expected median well As and F concentrations were calculated for the three pumping scenarios (Figures 5f and 5g) (Equation 12 in Table 2). Equation 12 in Table 2 predicts that median As and F concentrations will increase to 45 $\mu\text{g/L}$ and 3.4 mg/L, respectively, by 2120 under S1. The reviewed epidemiological dose-response studies (Hamadani et al., 2011; Wasserman et al., 2004, 2014) suggest that children consuming the present-day median As concentration of 14 $\mu\text{g/L}$ (over half the basin's population) will experience four IQ point reductions (Figure 5h). Under S1, IQ point decrements owing to As exposure are expected to increase to 6 by 2120 but the pumping scenarios do not have a strong impact on IQ point decrements from As owing to the flattening of the dose-response curve beyond current exposure levels (Figure 4a).

At current median F concentrations of 1 mg/L, only slight reductions in IQs are predicted (Figure 4b). By 2120, however, a wide range of IQ decrements from 4 to 12 points owing to childhood exposure to F concentrations are predicted (Figure 5g). This is caused by the steep dose-response curve (Figure 4b). We summed the separate predicted IQ decrements owing to exposure to As and F. Under S1, the population would be suffering a 19 point IQ decrement by 2120 (Figure 5j). The two lower pumping rate scenarios S2 and S3 would keep the population's IQ suppressed at approximately 12 and 9 points, respectively.

By the year 2120, owing to their reduced IQs, people living in the basin and drinking water from wells untreated under S1, S2, and S3 are expected to have median incomes of 2,609, 3,211, and 3,464 USD, respectively (Figure 5k). If, however, exposure was mitigated at no cost to the consumers, expected median incomes by 2120 rise to 4,174 USD (RO treatment in Figure 5k).

3.3. Economic Impacts of Pumping and Treatment Scenarios

The NPV of the increasing and decreasing pumping rate scenarios without and with drinking water quality mitigation was calculated relative to the NPV of the base case of constant pumping (S2) with no mitigation and assuming a 3% discount rate (Table 4). All calculations were performed assuming 1%, 3% and, 5% discount rates and the results are presented in Tables S2–S5 in Supporting Information S1 in 2020 dollars. The results in Table 4 are reported for the average crop value to water volume ratio (0.12 USD/m³) (weighted by irrigated water volume) (Table S1 in Supporting Information S1). These parameters are highly influential on the NPV results

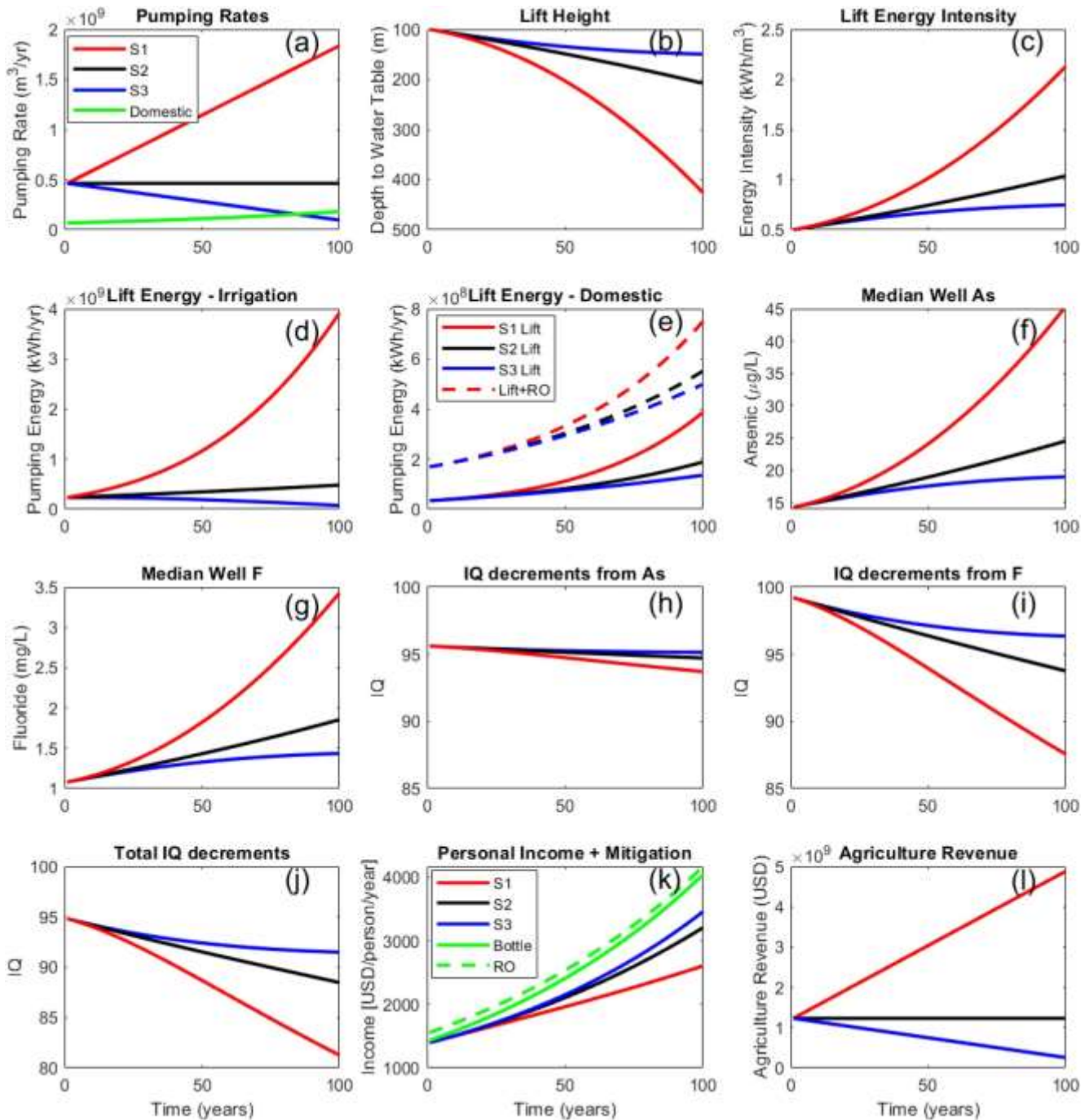


Figure 5. Impacts of future pumping rates on lift heights, energy demand, water quality, population IQ, and personal incomes. (a) Pumping rates for irrigation pumping scenarios and domestic pumping assuming a 1% population growth rate. (b) Expected lift heights. (c) Energy intensity required for lifting water to the surface. (d)

Energy demand for lifting irrigation water. (e) Energy demand for lifting domestic water (solid lines), and treating it using RO (dashed lines). (f) Expected median As and (g) F concentrations in wells water. (h) Individual impacts of As, (i) F, and (j) their combined impacts on the population IQ. (k) Expected growth in median personal income owing to IQ reduction or mitigation option chosen. (l) Growth or reduction in agriculture revenue. Simulation time-period is 100 years (2020–2120).

owing to the two order of magnitude variability of crop value to water ratio amongst crop types (Table S1 in Supporting Information S1, Table 3). The impacts of this variability and uncertainty on the reported NPV results were assessed in a sensitivity analysis (Section 3.4).

Table 4
Difference in Net Present Value (NPV) Analysis for Growing the Same Proportion of Crop Types Grown in 2020 Over Modeling Period (2020–2120) Assuming a 3% Discount Rate

Item	No Mitigation	Private Bottled Water	Community-Scale Mitigation
Agriculture Revenue:	1.44	1.44	1.44
Irrigation Population Costs:	-2.92	-2.92	-2.92
Domestic Population Costs:	-0.18	-0.18	-0.18
New Well	-0.65	-0.65	-0.65

D r i l i n g C o s t s :			
P e r s o n a l I n c o m e s :	-3.63	11.67	11.67
T r e a t m e n t C o s t s :	0.00	-4.10	-0.58
T o t a l N P V :	-5.96	5.25	8.77
A g R e v e n u e:	Base Case	0.00	0.00
I r r i g a t i o n P u m p i n g C o s t s :		0.00	0.00
D o		0.00	0.00

m e s t i c P u m p i n g C o s t s :			
N e w W e l l D r i l l i n g C o s t s :		0.00	0.00
P e r s o n a l I n c o m e s :		11.67	11.67
T r e a t m e n t C o s t s :		-4.10	-0.12
T o t a l N P V :		7.57	11.55
A g R e v e n	-0.38	-0.38	-0.38

u e:			
Irrigation Pumping Costs:	0.52	0.52	0.52
Domestic Pumping Costs:	0.05	0.05	0.05
New Well Drilling Costs:	0.06	0.06	0.06
Personal Income:	1.27	11.67	11.67
Treatment	0.00	-4.10	-0.54

ent Costs:			
Total NPV:	1.51	7.82	11.38

Note. The 2020 volume-weighted average revenue/water volume ratio was 0.12 (USD/m³) (Table S1 in Supporting Information S1). The differences in agriculture revenue, irrigation cost, domestic pumping cost, personal income, and drinking water mitigation costs are all calculated relative to the base case. All amounts are in units of 10⁹ USD in 2020. Hot and cool colors in the NPV boxes refer to less and greater value, respectively.

3.3.1. Economic Impacts of Varying Pumping Rates With No Drinking Water Quality Mitigation In the first column of Table 4, we compare the constant-pumping scenario (S2) with alternatives in which pumping increases gradually (S1) and decreases gradually (S3). Assuming farmers grew a portfolio of crops over the 100 years modeling period with a similar revenue per volume of irrigation water (0.12 USD/m³), the NPV generated from the sale of crops increases by 1.44 × 10⁹ USD under the increasing pumping scenario (S1). This increase in revenue, however, is more than offset by a 2.92 × 10⁹ USD increase in irrigation pumping costs and a 3.63 × 10⁹ USD reduction in household earnings owing to the additional exposure to As and F concentrations amongst the other more minor increases in expenses of additional domestic pumping (0.18 × 10⁹ USD) and new well installation costs (0.65 × 10⁹ USD). Hence, compared to S2, the relative NPV for S1 with no drinking water mitigation is −5.96 × 10⁹ USD.

If the irrigation pumping rate is slowly reduced over the next 100 years (S3), agricultural revenues are estimated to fall by 0.38 × 10⁹ USD compared to those of S2. This amount of lost revenue is smaller, however, than the 0.52 × 10⁹ USD decrease in irrigation pumping costs and the 1.27 × 10⁹ USD increase in household earnings owing to the relatively lower exposure to As and F compared to that of S2. Hence, relative NPV for S3 is 1.51 × 10⁹ USD.

3.3.2. Economic Impacts of Drinking Water Quality Mitigation

In the remaining columns of Table 4, we explore the relative economic impacts if bottled water or community-scale RO treatment is used to reduce exposure to As and F to negligible levels. Relative to the base case S2, in which we assume no mitigation of the As and F exposure levels, water treatment yields 11.67 × 10⁹ USD greater personal incomes. After subtracting the costs of bottled water and community-scaled RO treatment, the relative NPVs

Table 5
Difference in Net Present Value (NPV) Analysis for Growing Broccoli Over the Modeling Period (2020–2120) Assuming a 3% Discount Rate

	Item	No Mitigation	Private Bottled Water	Community-Scale Mitigation
Income:	Agriculture Revenue	18.50	18.50	18.50

n g (S 1)	Ir ri g a t i o n P u m p i n g C o s t s :	-2.92	-2.92	-2.92
	D o m e s t i c P u m p i n g C o s t s :	-0.18	-0.18	-0.18
	N e w W e l l D r i l l i n g C o s t s :	-0.65	-0.65	-0.65
	P e r s o n a l I n c o m e	-3.63	11.67	11.67

es :			
	0.00	-4.10	-0.58
T r e a t m e n t C o s t s :			
T o t a l N P V :	11.11	22.31	25.83
A g R e v e n u e:	Base Case	0.00	0.00
C o n s t a n t P u m p i n g (S 2)	Irrigation Consumption Pumping Costs:	0.00	0.00
	Domestic Pumping Costs:	0.00	0.00

Costs: New Well Drilling Costs: Personal Income: Treatment Costs: Total NPV: Reduced Pumping Irrigation			
		0.00	0.00
		11.67	11.67
		-4.10	-0.12
		7.57	11.55
		-4.93	-4.93
	0.52	0.52	0.52

(S 3)	g a t i o n P u m p i n g C o s t s :			
	D o m e s t i c P u m p i n g C o s t s :	0.05	0.05	0.05
	N e w W e l l D r i l l i n g C o s t s :	0.06	0.06	0.06
	P e r s o n a l I n c o m e s :	1.27	11.67	11.67

Treatment Costs:	0.00	-4.10	-0.54
Total NPV:	-3.04	3.27	6.83

Note. Broccoli has a Revenue/Water Volume Ratio of 1.5 (USD/m³) (Table S1 in Supporting Information S1). The differences in agriculture revenue, irrigation cost, domestic pumping cost, personal income, and drinking water mitigation costs are all calculated relative to the base case. All amounts are in units of 10⁹ USD in 2020. Hot and cool colors in the NPV boxes refer to less and greater value, respectively.

of these mitigations, while holding pumping constant, is 7.57×10^9 and 11.55×10^9 USD, respectively. This massive gain in value is predicted because such drastic lowering of exposures to negligible levels of As and F capitalizes on the large gains in IQ that occur at the low end of the dose-response curve.

If pumping increases over the next 100 years (S1) while implementing private bottled water, this results in a 5.25×10^9 USD greater NPV compared to that of S2 with no treatment. If community-scale RO treatment is utilized, this increases the difference in NPV to 8.77×10^9 USD. The scenarios with the greatest relative NPV are those in which pumping is reduced (S3) and private bottled water (7.82×10^9 USD) or community-scale RO treatment (11.38×10^9 USD) is used. This business-as-usual example illustrates that when a low value to water footprint crop is used, the magnitude of the gain in NPV from implementing drinking water treatment greatly exceeds that from increasing or reducing pumping.

3.3.3. Sensitivity of NPV to Variability in Crop Value

The low amount of revenue generated per volume of water by the 2020 portfolio of irrigated crops is the reason why the relative costs exceeded the benefits when irrigation pumping was increased relative to the base case. If, however, the water footprint and 2020 price for broccoli is assumed, with a revenue to water volume ratio of 1.5 (USD/m³), a large, positive relative NPV of 11.11×10^9 USD is calculated by increasing pumping (Table 5). The large, positive relative NPV from mitigating drinking water combines with the value added by increasing irrigation pumping to grow a high value, low water footprint crop. This results in a 25.83×10^9 USD relative NPV for community-scale mitigation with RO. In contrast, the relative NPV for the reduced pumping scenario (S3), when added to the benefits from drinking water mitigation using community-scale RO treatment, is still large and positive (6.83×10^9 USD), but it is smaller than the amount that assumes the lower value to water footprint crop (11.38×10^9 USD) (Table 4).

These results demonstrate that there is great opportunity to increase the revenue generated per water volume used in irrigation. In order for agriculture to generate enough revenue to offset the increased costs in irrigation and personal incomes (S1 vs. S2 in Table 4), a crop value to water footprint of 0.61 USD/m³ is required. The fifth through eighth most produced crops in 2020 (broccoli, asparagus, green chile, and tomatoes) all meet this criteria (Table S1 in Supporting Information S1, last column). If high value, low water footprint crops are grown, the overall revenue generated increases greatly, sufficient to offset the rising costs of energy to lift water to the surface. This is a cautionary note. Although high value crops offer farmers a way to earn higher income per volume of water, they create even greater incentives to overexploit the aquifer. Such a rebound effect has a precedent with the government-sponsored implementation of drip irrigation in this basin. The farmers were encouraged from the savings from energy costs since drip irrigation lowered the water footprint of their crops.

This improved the profitability of their operation, so they cultivated more land and ended up using more water (Hoogesteger & Wester, 2017). Thus, the intervention program increased revenue and profits for farms but did not conserve water.

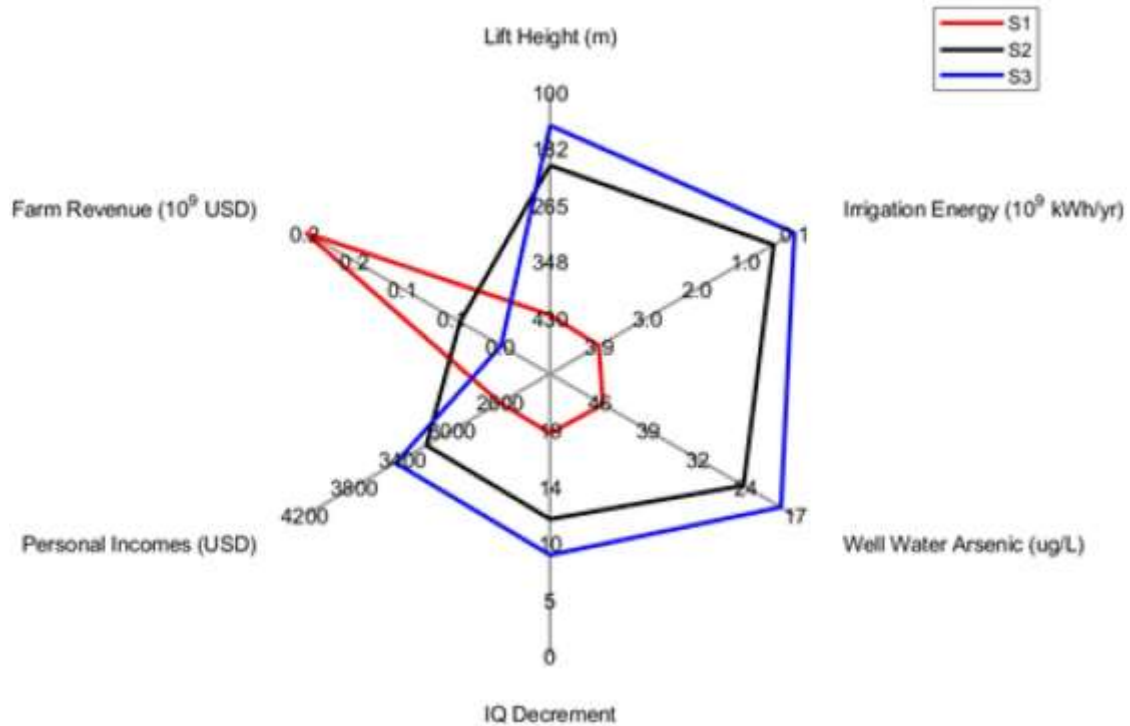
An alternative way to view the trade-offs available in this basin is to consider positive outcomes in the disparate domains of water quantity and quality, energy, human development, and economic and agricultural productivity as parameters to attempt to simultaneously optimize (Figure 6) (Jakeman & Letcher, 2003). The larger area in the radar plot indicates more positive outcomes from a given pumping or treatment scenario. More positive outcomes trend away from the center of the plot, leading to larger areas. Using this holistic approach, it suggests that the worst outcome is increasing pumping with no drinking water treatment (red area in Figure 6a), and the best outcome is from reduced pumping with treatment. This is the same conclusion that is drawn from the purely economic analysis in the case of the low value to water footprint crop (0.12 USD/m³) (Table 4), but contrasts with the economic findings when a higher value crop is chosen (1.51 USD/m³) (Table 5).

3.4. Limitations and Uncertainties of This Study

In this study, we do not calculate the negative impacts of diseases caused by exposure to As and F in drinking water. Although the present-day median concentrations are relatively low, the medians belie the high levels of exposure that some communities have been living with, where As and F concentrations range over 100 µg/L and 5 mg/L, respectively (Knappett et al., 2020). At these levels many serious diseases will result (Argos et al., 2010; Ayoob & Gupta, 2006); however, the comprehensive calculation of the health and economic impacts of these was beyond the scope of this study. This means that the relative NPV from mitigating exposure to As and F was underestimated. Second, it is beyond the scope of this study to model how agricultural revenue benefits the local population, but leaving the revenue in the benefits column (Table 4) assumes these revenue broadly benefit the local population through employment and wages. This is an overstatement of the value of that revenue to the households in this basin, however. Therefore, this study presents a more favorable picture of the net benefits (NPV) of overpumping the aquifer by agriculture than is likely to be the case. Third, we do not model how the improvement in health, which generally occurs with rising standards of living from economic growth, will help to reduce the impacts from exposure to As and F in drinking water. Improving schools, for example, can offset some of the IQ decrements suffered by exposure to neurotoxins.

There was considerable uncertainty or natural variability in 12 input parameters utilized in the model (Table 3). These parameters are grouped into hydrological (P , I/P , H_t , z_o , S_y), geochemical (k_{As} , k_F), epidemiologic (β_{As} , β_F), economic (R_{IQ}), and agricultural (s , P_{crop}) categories. These parameters were varied across (a) their entire range, in the case of parameters with few estimates; (b) their 95% Confidence Interval (C.I.), in the case of fitted parameters; (c) their inter-quartile range, in the case of a large number of possible values; (d) and $\pm 25\%$ of the parameter value, in the case of poorly constrained uncertainty or variability. The sensitivity of 15 key output parameters to the variability or uncertainty in these 12 input parameters were evaluated (Figure S12 in Supporting Information S1). The largest and broadest sensitivity in output parameters were generated from hydrologic parameters. This is partly because the hydrology components of the model are upstream of the other components, which drives a cascading effect. Human development and economic output parameters were relatively insensitive to variation in the As-depth gradient (k_{As}) and the coefficient of the dose-response curve (β_{As}) owing to the fact that

(a) No Drinking Water Mitigation



(b) With Drinking Water Mitigation

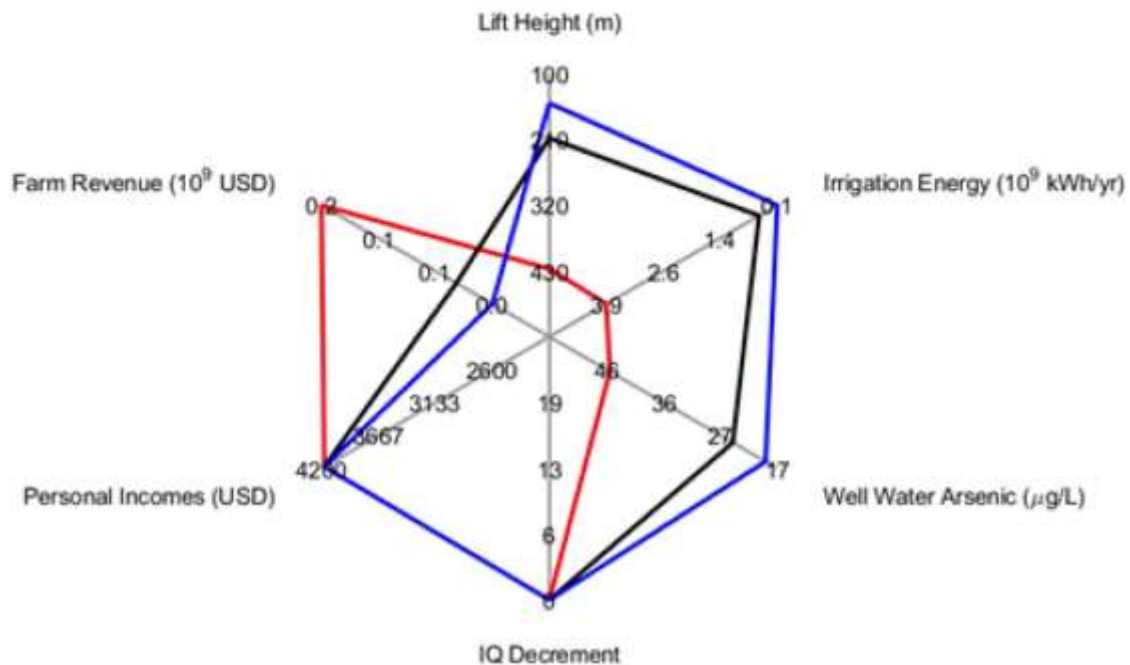


Figure 6. Radar plots showing relative benefits of pumping scenarios without (a) and with (b) drinking water quality mitigation. Benefits are greater in the outward direction, whereas costs are greater in the inward direction. The amount represent annual values in the year 2120. Monetary units are not discounted and the crop value per water footprint ratio is the volume-weighted average of 2020 (0.12 USD/m³).

present-day median As concentrations are already located on the relatively flat part of the dose-response curve (Figure 4a). In contrast, the F-depth gradient (k_F) is influential on these output parameters owing to the shape of its dose-response curve (Figure 4b). As highlighted already, agriculture revenue is highly sensitive to the large range of crop values and crop water footprints.

3.5. Opportunities for Improvement of Models of the Food-Water-Energy-Health Nexus

The revenue generated from growing food for export out of the basin dominates over energy costs when a high value, low water footprint crop is grown. The actual water footprints for this region are not known, however. Although the literature values used herein provide a baseline, metering, remote sensing, or field observations of ET could provide more specific values. Cloud cover in this semiarid region is limited, and since metering is either absent or not trustworthy, satellite based methods are promising. These can be constrained by reliable documentation of plantings and harvests from the Mexican Agri-food and Fishing Information Service (SIAP) as well as standard Food and Agriculture Organization methods to calculate the water demand for given crop types according to their climate (Allen et al., 1998). From these data, the volume of water embedded in crop production could be linked to either the tonnes of crops produced or to the dollar value of that production (Hoekstra et al., 2011; Hoekstra & Mekonnen, 2012). Preliminary work by our group has established these relationships for Mexico at the county scale (Torres Padilla, 2021). Adding such an analysis is important for characterizing the impacts of agricultural planting behaviors, as farmers will tend to respond to market prices for foods. If a crop type with high water demand is also highly profitable to grow and export, this will increase pumping. Therefore, the response of irrigation pumping to global market swings in foods could be explicitly modeled and constrained by historical data using the nation-wide crop-rotation database.

Irrigation efficiency was not explicitly considered in this model, although flood, spigot, and drip irrigation technologies are all widely deployed across the basin. The state and federal governments have subsidized a shift toward drip irrigation, but this was met with mixed success as mentioned. Therefore, a future model could also explore how crop profitability, as a function of market prices and irrigation technique, leads to greater or less irrigation pumping.

This study highlights the vast human potential in earnings that could be unleashed by reducing exposure to As and F concentrations in the drinking water. The NPV of this rivals the value of switching to growing high value, low water footprint crops (Table 5).

4. Conclusions

Polluting industries that impose costs on populations living near them is nothing new. Our study is novel because we link the activity of overexploiting an aquifer, which is seen as a water supply problem, to human health and economic development in the broader population. In a semiarid region, the quantity and quality of groundwater is the natural heritage of the population who lives above the aquifer. We quantify the diminishing value of that heritage to the local population over time by calculating how much it will cost to access and treat (or not treat) this water that is now contaminated.

This study does not ignore the benefits from agriculture. Rather, the model overstates the benefit of irrigation pumping and agricultural production to the residents in the basin, since much of the benefits of farming go to owners, shareholders, and consumers who do not live in the basin. Even after including the benefits of pumping more groundwater for irrigation, the rising electricity costs and worsening As and F concentrations means that pumping at higher rates than today will reduce the NPV of the basin's agricultural industry and the incomes of the people who live there. This could be addressed by growing higher value, lower water footprint crops (through either crop type or through improved irrigation efficiency), but even in the highest revenue-generating scenarios where only one of the highest value, lowest water footprint crops are assumed to be grown across the basin (broccoli), the benefit of reducing human exposure to As and F is roughly equal to the entire revenue generated by the agriculture industry in this basin.

Removing environmental exposures to neurotoxins (not to mention carcinogens) is an achievable step in developing a nation's human resources. Doing this weakens positive feedback loops that drive intergenerational poverty.

Acknowledgments

The authors are grateful to Manuel Aviles and many other students from the University of Guanajuato for assisting in field work. Funding was provided by the Texas A&M University – CONACYT collaborative research grant program (Grant Nos. 2014-001 and 2017-034s) and the Universidad de Guanajuato (Grant Nos. 004/2015 and 1013/2016). The authors thank two anonymous reviewers who greatly improved the quality of the manuscript.

Our study shows that blanket treatment of water to remove As and F in this region will have a similar economic impact on the region as would a highly performing agriculture industry.

Although aquifers in productive agricultural regions in the developing world are commonly under-characterized, there are growing databases on water levels and water quality that could be used to reveal the linkages between pumping, drawdown, and geogenic contaminants in the remaining groundwater. Whereas water tables tend to decline in a linear way, exponential relationships in groundwater chemistry with depth and dose-response curves for exposure to geogenic contaminants are common. These multiple nonlinear relationships acting on each other impact aquifers, energy, human health, and economics. Designing experiments to parameterize the linkages in hydro-health-economic models is all the more pressing under climate change, which will make semiarid regions like central Mexico dryer and hotter, leading to higher demand for irrigation pumping.

Conflict of Interest

The authors declare no conflicts of interest relevant to this study.

Data Availability Statement

Additional figures, data, and the modeling code that is the presented model are provided in Supporting Information S1. All well water chemistry data that were utilized in this study can be found at: <https://doi.org/10.4211/hs.d43fad1af0c642b697650d2aa979f29d>. All well construction, electricity costs, pumping rates and schedules, and numbers of households served can be found at: <https://doi.org/10.4211/hs.d97ce5c11dc347f49a4ec474199dd331>. Each database can be easily cross-referenced using the well ID.

References

- Alarcon-Herrera, M. T., Bundschuh, J., Nath, B., Nicolli, H. B., Gutierrez, M., Reyes-Gomez, V. M., et al. (2013). Co-occurrence of arsenic and fluoride in groundwater of semi-arid regions in Latin America: Genesis, mobility and remediation. *Journal of Hazardous Materials*, 262, 960–969. <https://doi.org/10.1016/j.jhazmat.2012.08.005>
- Alarcon-Herrera, M. T., Martin-Alarcon, D. A., Gutierrez, M., Reynoso-Cuevas, L., Martin-Dominguez, A. M., Olmos-Marquez, M. A., & Bundschuh, J. (2019). Co-occurrence, possible origin, and health-risk assessment of arsenic and fluoride in drinking water sources in Mexico: Geographical data visualization. *Science of the Total Environment*, 698, 134168. <https://doi.org/10.1016/j.scitotenv.2019.134168>
- Alcala, F. J., & Custodio, E. (2008). Using the Cl/Br ratio as a tracer to identify the origin of salinity in aquifers in Spain and Portugal. *Journal of Hydrology*, 359(1–2), 189–207. <https://doi.org/10.1016/j.jhydrol.2008.06.028>
- Allen, R. G., Pereira, L. S., & Raes, D. (1998). *Crop evapotranspiration-Guidelines for computing crop water requirements-FAO Irrigation and drainage*. Food and Agriculture Organization.
- Amini, M., Abbaspour, K. C., Berg, M., Winkel, L., Hug, S. J., Hoehn, E., et al. (2008). Statistical modeling of global geogenic arsenic contamination in groundwater. *Environmental Science & Technology*, 42(10), 3669–3675. <https://doi.org/10.1021/es702859e>
- Amini, M., Mueller, K., Abbaspour, K. C., Rosenberg, T., Afyuni, M., Moller, K. N., et al. (2008). Statistical modeling of global geogenic fluoride contamination in groundwaters. *Environmental Science & Technology*, 42(10), 3662–3668. <https://doi.org/10.1021/es071958y>
- Argos, M., Kalra, T., Rathouz, P. J., Chen, Y., Pierce, B., Parvez, F., et al. (2010). Arsenic exposure from drinking water, and all-cause and chronic-disease mortalities in Bangladesh (HEALS): A prospective cohort study. *Lancet*, 376(9737), 252–258. [https://doi.org/10.1016/s0140-6736\(10\)60481-3](https://doi.org/10.1016/s0140-6736(10)60481-3)
- Attina, T. M., & Trasande, L. (2013). Economic costs of childhood lead exposure in low- and middle-income countries. *Environmental Health Perspectives*, 121(9), 1097–1102. <https://doi.org/10.1289/ehp.1206424>
- Ayoob, S., & Gupta, A. K. (2006). Fluoride in drinking water: A review on the status and stress effects. *Critical Reviews in Environmental Science and Technology*, 36(6), 433–487. <https://doi.org/10.1080/10643380600678112>
- Ayotte, J. D., Belaval, M., Olson, S. A., Burow, K. R., Flanagan, S. M., Hinkle, S. R., & Lindsey, B. D. (2015). Factors affecting temporal variability of arsenic in groundwater used for drinking water supply in the United States. *Science of the Total Environment*, 505, 1370–1379. <https://doi.org/10.1016/j.scitotenv.2014.02.057>
- Ayotte, J. D., Szabo, Z., Focazio, M. J., & Eberts, S. M. (2011). Effects of human-induced alteration of groundwater flow on concentrations of naturally-occurring trace elements at water-supply wells. *Applied Geochemistry*, 26(5), 747–762. <https://doi.org/10.1016/j.apgeochem.2011.01.033>
- Bashash, M., Thomas, D., Hu, H., Martinez-Mier, E. A., Sanchez, B. N., Basu, N., et al. (2017). Prenatal fluoride exposure and cognitive outcomes in children at 4 and 6–12 years of age in Mexico. *Environmental Health Perspectives*, 125(9), 097017. <https://doi.org/10.1289/ehp655>
- Boden, K. S., & Subban, C. V. (2018). *A road map for small-scale desalination* (p. 68). OXFAM.
- Bundschuh, J., Litter, M., Ciminelli, V. S. T., Morgada, M. E., Cornejo, L., Hoyos, S. G., et al. (2010). Emerging mitigation needs and sustainable options for solving the arsenic problems of rural and isolated urban areas in Latin America – A critical analysis. *Water Research*, 44(19), 5828–5845. <https://doi.org/10.1016/j.watres.2010.04.001>
- Bustingorri, C., & Lavado, R. S. (2014). Soybean as affected by high concentrations of arsenic and fluoride in irrigation water in controlled conditions. *Agricultural Water Management*, 144, 134–139. <https://doi.org/10.1016/j.agwat.2014.06.004>
- Cai, X. M. (2008). Implementation of holistic water resources-economic optimization models for river basin management – Reflective experiences. *Environmental Modelling & Software*, 23(1), 2–18. <https://doi.org/10.1016/j.envsoft.2007.03.005>

Carter, N. T., & Nesbitt, A. C. (2016). *Discount rates in the economic evaluation of US Army Corps of Engineers projects* (C. R. Service, Ed.). Congressional Research Service.

- Castro, C., Corbo-Camargo, F., & Loza-Aguirre, I. (2021). Geophysical model of Cuenca de la Independencia aquifer. *Journal of Applied Geophysics*, 186, 104257. <https://doi.org/10.1016/j.jappgeo.2021.104257>
- Choi, A. L., Sun, G. F., Zhang, Y., & Grandjean, P. (2012). Developmental fluoride neurotoxicity: A systematic review and meta-analysis. *Environmental Health Perspectives*, 120(10), 1362–1368. <https://doi.org/10.1289/ehp.1104912>
- Choi, A. L., Zhang, Y., Sun, G. F., Bellinger, D. C., Wang, K. L., Yang, X. J., et al. (2015). Association of lifetime exposure to fluoride and cognitive functions in Chinese children: A pilot study. *Neurotoxicology and Teratology*, 47, 96–101. <https://doi.org/10.1016/j.ntt.2014.11.001>
- Cidu, R., Frau, F., & Tore, P. (2011). Drinking water quality: Comparing inorganic components in bottled water and Italian tap water. *Journal of Food Composition and Analysis*, 24(2), 184–193. <https://doi.org/10.1016/j.jfca.2010.08.005>
- Clark, I., & Fritz, P. (1997). *Environmental isotopes in hydrogeology*. CRC Press.
- CONAGUA. (2007). *Manual de agua potable, alcantarillado y saneamiento*. Comisión Nacional del Agua.
- CONAGUA. (2020a). *Actualización de la Disponibilidad Media Anual de Agua en el Acuífero Cuenca Alta del Río Laja (1108) Estado de Guanajuato* (p. 42). Comisión Nacional del Agua.
- CONAGUA. (2020b). *Actualización de la Disponibilidad Media Anual de Agua en el Acuífero Doctor Mora-San José Iturbide (1106), Estado de Guanajuato* (p. 32). Comisión Nacional del Agua.
- CONAGUA. (2020c). *Actualización de la Disponibilidad Media Anual de Agua en el Acuífero Laguna Seca (1104) Estado de Guanajuato* (p. 43). Comisión Nacional del Agua.
- CONAGUA. (2020d). *Actualización de la Disponibilidad Media Anual de Agua en el Acuífero San Miguel de Allende (1107) Estado de Guanajuato*. Comisión Nacional del Agua.
- CONAGUA. (2020e). *Registro Público de Derechos de Agua (REPGA)*. Mexican Federal Government.
- Consultores en Geología, S. A. d. C. V. (1992). *Modelo Matemático de la Cuenca Alta del Río de la Laja*. Comisión Nacional del Agua.
- Cruz, A. O. I., Alvarez-Chavez, C. R., Ramos-Corella, M. A., & Soto-Hernandez, F. (2017). Determinants of domestic water consumption in Hermosillo, Sonora, Mexico. *Journal of Cleaner Production*, 142, 1901–1910. <https://doi.org/10.1016/j.jclepro.2016.11.094>
- Del Pilar-Martínez, A., Nieto-Samaniego, A. F., Alaniz-Alvarez, S. A., & Angeles-Moreno, E. (2020). Geology of the southern mesa central of Mexico: Recording the beginning of a polymodal fault system. *Journal of Maps*, 16(2), 199–211. <https://doi.org/10.1080/17445647.2020.1719911>
- Del Razo, L. M., Ledon, J. M., & Velasco, M. N. (2018). *Arsenico y fluoruro en agua: Riesgos y perspectivas desde la sociedad civil y la academia en Mexico* (p. 202). Secretaría de Gobernación.
- Del Rio, P., Nieto-Samaniego, A. F., Alaniz-Alvarez, S. A., Angeles-Moreno, E., Escalona-Alcazar, F., & Del Pilar-Martínez, A. (2020). Geología y estructura de las sierras de Guanajuato y Cordones, Mexa Central, Mexico. *Boletín de la Sociedad Geológica Mexicana*, 72(1), A071019.
- Desai, G., Barg, G., Vahter, M., Queirolo, E. I., Peregalli, F., Manay, N., et al. (2020). Executive functions in school children from Montevideo, Uruguay and their associations with concurrent low-level arsenic exposure. *Environment International*, 142, 105883. <https://doi.org/10.1016/j.envint.2020.105883>
- Elshafei, Y., Coletti, J. Z., Sivapalan, M., & Hipsey, M. R. (2015). A model of the socio-hydrologic dynamics in a semiarid catchment: Isolating feedbacks in the coupled human-hydrology system. *Water Resources Research*, 51(8), 6442–6471. <https://doi.org/10.1002/2015wr017048>
- Fulton, J., Norton, M., & Shilling, F. (2019). Water-indexed benefits and impacts of California almonds. *Ecological Indicators*, 96, 711–717. <https://doi.org/10.1016/j.ecolind.2017.12.063>
- Grandjean, P., & Landrigan, P. J. (2006). Developmental neurotoxicity of industrial chemicals. *Lancet*, 368(9553), 2167–2178. [https://doi.org/10.1016/s0140-6736\(06\)69665-7](https://doi.org/10.1016/s0140-6736(06)69665-7)
- Green, J. (2018). Bottled water in Mexico: The rise of a new access to water paradigm. *WIREs Water*, 5, e1286. <https://doi.org/10.1002/wat2.1286>
- Grosse, S. D., Matte, T. D., Schwartz, J., & Jackson, R. J. (2002). Economic gains resulting from the reduction in children's exposure to lead in the United States. *Environmental Health Perspectives*, 110(6), 563–569. <https://doi.org/10.1289/ehp.02110563>
- Guo, Q. H., Wang, Y. X., & Liu, W. (2008). B, As, and F contamination of river water due to wastewater discharge of the Yangbajing geothermal power plant, Tibet, China. *Environmental Geology*, 56(1), 197–205. <https://doi.org/10.1007/s00254-007-1155-2>
- Hamadani, J. D., Tofail, F., Nermell, B., Gardner, R., Shiraji, S., Bottai, M., et al. (2011). Critical windows of exposure for arsenic-associated impairment of cognitive function in pre-school girls and boys: A population-based cohort study. *International Journal of Epidemiology*, 40(6), 1593–1604. <https://doi.org/10.1093/ije/dyr176>
- Harou, J. J., & Lund, J. R. (2008). Ending groundwater overdraft in hydrologic-economic systems. *Hydrogeology Journal*, 16(6), 1039–1055. <https://doi.org/10.1007/s10040-008-0300-7>
- Harou, J. J., Pulido-Velazquez, M., Rosenberg, D. E., Medellín-Azuara, J., Lund, J. R., & Howitt, R. E. (2009). Hydro-economic models: Concepts, design, applications, and future prospects. *Journal of Hydrology*, 375(3–4), 627–643. <https://doi.org/10.1016/j.jhydrol.2009.06.037>
- Hoekstra, A. Y., Chapagain, A. K., Aldaya, M. M., & Mekonnen, M. M. (2011). *The water footprint assessment manual: Setting the global standard*. Routledge.
- Hoekstra, A. Y., & Mekonnen, M. M. (2012). The water footprint of humanity. *Proceedings of the National Academy of Sciences of the United States of America*, 109(9), 3232–3237. <https://doi.org/10.1073/pnas.1109936109>
- Hoogesteger, J., & Wester, P. (2017). Regulating groundwater use: The challenges of policy implementation in Guanajuato, Central Mexico. *Environmental Science & Policy*, 77, 107–113. <https://doi.org/10.1016/j.envsci.2017.08.002>
- Howard, B. C. (2014, August 16). *California drought spurs groundwater drilling boom in Central Valley*. National Geographic. <https://www.nationalgeographic.com/culture/article/140815-central-valley-california-drilling-boom-groundwater-drought-wells>
- INEGI. (2021, September 20). *Instituto Nacional de Estadística y Geografía (INEGI)*. http://cuentame.inegi.org.mx/monografias/informacion/gto/territorio/div_municipal.aspx?t
- Ingenieros Civiles y Geólogos Asociados, S. A. (1980). *Estudio Geohidrológico en el Valle de San José Iturbide* (Report No. 1751).
- Izbicki, J. A., Teague, N. F., Hatzinger, P. B., Bohlke, J. K., & Sturchio, N. C. (2015). Groundwater movement, recharge, and perchlorate occurrence in a faulted alluvial aquifer in California (USA). *Hydrogeology Journal*, 23(3), 467–491. <https://doi.org/10.1007/s10040-014-1217-y>
- Jakeman, A. J., & Letcher, R. A. (2003). Integrated assessment and modelling: Features, principles and examples for catchment management. *Environmental Modelling & Software*, 18(6), 491–501. [https://doi.org/10.1016/s1364-8152\(03\)00024-0](https://doi.org/10.1016/s1364-8152(03)00024-0)
- Knappett, P. S. K., Li, Y., Loza, I., Hernandez, H., Aviles, M., Haaf, D., et al. (2020). Rising arsenic concentrations from dewatering a geothermally influenced aquifer in central Mexico. *Water Research*, 185(116257), 116257. <https://doi.org/10.1016/j.watres.2020.116257>

- Knappett, P. S. K., Li, Y. M., Hernandez, H., Rodriguez, R., Aviles, M., Deng, C., et al. (2018). Changing recharge pathways within an intensively pumped aquifer with high fluoride concentrations in Central Mexico. *Science of the Total Environment*, 622, 1029–1045. <https://doi.org/10.1016/j.scitotenv.2017.12.031>
- LaFayette, G. N., Knappett, P. S. K., Li, Y., Loza-Aguirre, I., & Polizzotto, M. L. (2020). Geogenic sources and chemical controls on fluoride release to groundwater in the Independence Basin, Mexico. *Applied Geochemistry*, 123, 104787. <https://doi.org/10.1016/j.apgeochem.2020.104787>
- Lefkoff, L. J., & Gorelick, S. M. (1990). Simulating physical processes and economic-behavior in saline, irrigated agriculture – Model development. *Water Resources Research*, 26(7), 1359–1369. <https://doi.org/10.1029/wr026i007p01359>
- Li, Y. M., Hernandez, J. H., Aviles, M., Knappett, P. S. K., Giardino, J. R., Miranda, R., et al. (2020). Empirical Bayesian Kriging method to evaluate inter-annual water-table evolution in the Cuenca Alta del Rio Laja aquifer, Guanajuato, Mexico. *Journal of Hydrology*, 582, 124517. <https://doi.org/10.1016/j.jhydrol.2019.124517>
- Loza-Aguirre, I., Nieto-Samaniego, A. F., Alaniz-Alvarez, S. A., & Ortega-Guerrero, M. A. (2012). Cenozoic volcanism and extension in northwestern mesa central, Durango, Mexico. *Boletín De La Sociedad Geologica Mexicana*, 64(2), 243–263. <https://doi.org/10.18268/bsgm2012v64n2a9>
- Mahlknecht, J., Schneider, J., Merkel, B., deLeon, I. N., & Bernasconi, S. (2004). Groundwater recharge in a sedimentary basin in semi-arid Mexico. *Hydrogeology Journal*, 12(5), 511–530. <https://doi.org/10.1007/s10040-004-0332-6>
- Mayo, A. L. (2010). Ambient well-bore mixing, aquifer cross-contamination, pumping stress, and water quality from long-screened wells: What is sampled and what is not? *Hydrogeology Journal*, 18(4), 823–837. <https://doi.org/10.1007/s10040-009-0568-2>
- Mekonnen, M. M., & Hoekstra, A. Y. (2011). The green, blue and grey water footprint of crops and derived crop products. *Hydrology and Earth System Sciences*, 15(5), 1577–1600. <https://doi.org/10.5194/hess-15-1577-2011>
- Mekonnen, M. M., & Hoekstra, A. Y. (2013). *Water footprint benchmarks for crop production*. UNESCO-IHE Institute for Water Education.
- Morales-Arredondo, J. I., Esteller-Alberich, M. V., Hernandez, M. A. A., & Martinez-Florentino, T. A. K. (2018). Characterizing the hydrogeochemistry of two low-temperature thermal systems in Central Mexico. *Journal of Geochemical Exploration*, 185, 93–104. <https://doi.org/10.1016/j.gexplo.2017.11.006>
- Nahar, M. N., Inaoka, T., & Fujimura, M. (2014). A consecutive study on arsenic exposure and intelligence quotient (IQ) of children in Bangladesh. *Environmental Health and Preventive Medicine*, 19(3), 194–199. <https://doi.org/10.1007/s12199-013-0374-2>
- Nordstrom, D. K. (2002). Public health – Worldwide occurrences of arsenic in ground water. *Science*, 296(5576), 2143–2145. <https://doi.org/10.1126/science.1072375>
- Nowicki, S., Koehler, J., & Charles, K. J. (2020). Including water quality monitoring in rural water services: Why safe water requires challenging the quantity versus quality dichotomy. *Npj Clean Water*, 3(1), 1–9. <https://doi.org/10.1038/s41545-020-0062-x>
- Oropeza-Perez, I., & Petzold-Rodriguez, A. H. (2018). Analysis of the energy use in the Mexican residential sector by using two approaches regarding the behavior of the occupants. *Applied Sciences-Basel*, 8(11), 2136. <https://doi.org/10.3390/app8112136>
- Ortega-Guerrero, M. A. (2009). Occurrence, distribution, hydrochemistry and origin of arsenic, fluoride and other trace elements dissolved in groundwater at basin scale in central Mexico. *Revista Mexicana de Ciencias Geológicas*, 26(1), 143–161.
- Ostrom, E. (1990). *Governing the commons: The evolution of institutions for collective action*. Cambridge University Press.
- Podgorski, J. E., Eqani, S. A. M. A. S., Khanam, T., Ullah, R., Shen, H. Q., & Berg, M. (2017). Extensive arsenic contamination in high-pH unconfined aquifers in the Indus Valley. *Science Advances*, 3(8), e1700935. <https://doi.org/10.1126/sciadv.1700935>
- Podgorski, J. E., Labhasetwar, P., Saha, D., & Berg, M. (2018). Prediction modeling and mapping of groundwater fluoride contamination throughout India. *Environmental Science & Technology*, 52(17), 9889–9898. <https://doi.org/10.1021/acs.est.8b01679>
- Pratap, D., & Singh, D. (2013). Impact of fluoride on environment and human health. *Pratibha: International Journal of Science, Spirituality, Business and Technology*, 1(2), 2277–2261.
- Prol-Ledesma, R. M., & Moran-Zenteno, D. J. (2019). Heat flow and geothermal provinces in Mexico. *Geothermics*, 78, 183–200. <https://doi.org/10.1016/j.geothermics.2018.12.009>
- Rango, T., Bianchini, G., Beccaluva, L., & Tassinari, R. (2010). Geochemistry and water quality assessment of central Main Ethiopian Rift natural waters with emphasis on source and occurrence of fluoride and arsenic. *Journal of African Earth Sciences*, 57(5), 479–491. <https://doi.org/10.1016/j.jafrearsci.2009.12.005>
- Rango, T., Vengosh, A., Dwyer, G., & Bianchini, G. (2013). Mobilization of arsenic and other naturally occurring contaminants in groundwater of the Main Ethiopian Rift aquifers. *Water Research*, 47(15), 5801–5818. <https://doi.org/10.1016/j.watres.2013.07.002>
- Reyes-Gomez, V. M., Alarcon-Herrera, M. T., Gutierrez, M., & Lopez, D. N. (2013). Fluoride and arsenic in an alluvial aquifer system in Chihuahua, Mexico: Contaminant levels, potential sources, and co-occurrence. *Water, Air, and Soil Pollution*, 224(2), 1–15. <https://doi.org/10.1007/s11270-013-1433-4>
- Rocha-Amador, D., Navarro, M. E., Carrizales, L., Morales, R., & Calderon, J. (2007). Decreased intelligence in children and exposure to fluoride and arsenic in drinking water. *Cadernos de Saude Pública*, 23, S579–S587. <https://doi.org/10.1590/s0102-311x2007001600018>
- Rodriguez-Barranco, M., Lacasana, M., Aguilar-Garduno, C., Alguacil, J., Gil, F., Gonzalez-Alzaga, B., & Rojas-Garcia, A. (2013). Association of arsenic, cadmium and manganese exposure with neurodevelopment and behavioural disorders in children: A systematic review and meta-analysis. *Science of the Total Environment*, 454, 562–577. <https://doi.org/10.1016/j.scitotenv.2013.03.047>
- Rosin-Grget, K., Peros, K., Sutej, I., & Basic, K. (2013). The cariostatic mechanisms of fluoride. *Acta Medica Academica*, 42(2), 179–188. <https://doi.org/10.5644/ama2006-124.85>
- Saeed, M., Rehman, M. Y. A., Farooqi, A., & Malik, R. N. (2021). *Arsenic and fluoride co-exposure through drinking water and their impacts on intelligence and oxidative stress among rural school-aged children of Lahore and Kasur districts, Pakistan*. Environmental Geochemistry and Health.
- Sage, A. P., Minatel, B. C., Ng, K. W., Stewart, G. L., Dummer, T. J. B., Lam, W. L., & Martinez, V. D. (2017). Oncogenomic disruptions in arsenic-induced carcinogenesis. *Oncotarget*, 8(15), 25736–25755. <https://doi.org/10.18632/oncotarget.15106>
- Schwartz, J., Pitcher, H., Levin, R., Ostro, B., & Nichols, A. L. (1985). *Costs and benefits of reducing lead in gasoline: Final regulatory impact analysis* (p. 495). United States Environmental Protection Agency.
- Scott, C. A. (2011). The water-energy-climate nexus: Resources and policy outlook for aquifers in Mexico. *Water Resources Research*, 47(6), W00L04. <https://doi.org/10.1029/2011wr010805>
- Sedlak, D. L. (2019). The unintended consequences of the reverse osmosis revolution. *Environmental Science & Technology*, 53(8), 3999–4000. <https://doi.org/10.1021/acs.est.9b01755>
- SENER. (2018). *Prospectiva del Sector Eléctrico 2018–2032* (p. 145). Secretaría de Energía.

- Shepherd, F. T. (2018). *Arsenic and fluoride contamination in the independence Basin aquifer system of Guanajuato*. Kansas State University.
- SIAP. (2020, September 8). *Estadística de Producción Agrícola*. http://infosiap.siap.gob.mx/gobmx/datosAbiertos_a.php
- Signes-Pastor, A. J., Vioque, J., Navarrete-Munoz, E. M., Carey, M., Garcia-Villarino, M., Fernandez-Somoano, A., et al. (2019). Inorganic arsenic exposure and neuropsychological development of children of 4–5 years of age living in Spain. *Environmental Research*, *174*, 135–142. <https://doi.org/10.1016/j.envres.2019.04.028>
- Smedley, P. L., & Kinniburgh, D. G. (2002). A review of the source, behaviour and distribution of arsenic in natural waters. *Applied Geochemistry*, *17*(5), 517–568. [https://doi.org/10.1016/s0883-2927\(02\)00018-5](https://doi.org/10.1016/s0883-2927(02)00018-5)
- Smith, R., Knight, R., & Fendorf, S. (2018). Overpumping leads to California groundwater arsenic threat. *Nature Communications*, *9*, 2089. <https://doi.org/10.1038/s41467-018-04475-3>
- Srinivasan, V., Gorelick, S. M., & Goulder, L. (2010). A hydrologic-economic modeling approach for analysis of urban water supply dynamics in Chennai, India. *Water Resources Research*, *46*(7), W07540. <https://doi.org/10.1029/2009wr008693>
- Stern, N. H. (2007). *The economics of climate change: The stern review*. Cambridge University Press.
- Till, C., & Green, R. (2021). Controversy: The evolving science of fluoride: When new evidence doesn't conform with existing beliefs. *Pediatric Research*, *90*(5), 1093–1095. <https://doi.org/10.1038/s41390-020-0973-8>
- Torres Padilla, E. (2021). *Embedded water in agricultural goods for sustainable water use in Mexico*. Texas A&M University.
- US EPA. (2019). *Work breakdown structure-based cost model for reverse osmosis/nanofiltration drinking water treatment*. US EPA.
- Vahter, M., Skroder, H., Rahman, S. M., Levi, M., Hamadani, J. D., & Kippler, M. (2020). Prenatal and childhood arsenic exposure through drinking water and food and cognitive abilities at 10 years of age: A prospective cohort study. *Environment International*, *139*, 105723. <https://doi.org/10.1016/j.envint.2020.105723>
- Wasserman, G. A., Liu, X. H., Lolocono, N. J., Kline, J., Factor-Litvak, P., van Geen, A., et al. (2014). A cross-sectional study of well water arsenic and child IQ in Maine schoolchildren. *Environmental Health*, *13*, 23. <https://doi.org/10.1186/1476-069x-13-23>
- Wasserman, G. A., Liu, X. H., Parvez, F., Ahsan, H., Factor-Litvak, P., vanGeen, A., et al. (2004). Water arsenic exposure and children's intellectual function in Araihazar, Bangladesh. *Environmental Health Perspectives*, *112*(13), 1329–1333. <https://doi.org/10.1289/ehp.6964>
- Wasserman, G. A., Liu, X. H., Parvez, F., Factor-Litvak, P., Kline, J., Siddique, A. B., et al. (2016). Child intelligence and reductions in water arsenic and manganese: A two-year follow-up study in Bangladesh. *Environmental Health Perspectives*, *124*(7), 1114–1120. <https://doi.org/10.1289/ehp.1509974>
- Weiner, R. F., & Matthews, R. A. (2003). *Environmental engineering*. Butterworth-Heinemann.
- WHO. (2019). *Exposure to inadequate or excess fluoride: A major public health concern*. World Health Organization.
- Xing, S. P., Guo, H. M., Zhang, L. Z., Wang, Z., & Sun, X. M. (2022). Silicate weathering contributed to arsenic enrichment in geotherm-affected groundwater in Pliocene aquifers of the Guide basin, China. *Journal of Hydrology*, *606*, 127444. <https://doi.org/10.1016/j.jhydrol.2022.127444>

References From the Supporting Information

- Mahlknecht, J. (2003). *Estimation of recharge in the Independence aquifer, central Mexico, by combining geochemical and groundwater flow models*. University of Agricultural and Life Sciences (BOKU).